Table 1. Cont.

The Huh7.25.CD81 cells, seeded at 3.10^6 cells in 10-cm plates, were transfected after 24 hrs with 25 nM of siRNA Control or siRNA PKR using Fugene HD. 24 hrs post transfection, they were either mock-infected or infected for 2 hrs at 37°C with JFH1 (moi = 0.2) (three independent plates/sample). The medium was then removed and cells were incubated with complete DMEM for 12 hrs at 37°C. The cells were washed twice with TBS containing phosphatase and protease inhibitors, harvested by scraping, the cell pellets were centrifuged, the supernatants were removed and the pellets were frozen and stored at −80°C before being processed for micro-array.The list shows genes that were affected no more than twice by the depletion of PKR in the control cells ($0.5<$ siPKR mock/siCt <1.6). The dependence of each of these genes in regards with PKR for their induction by HCV is expressed as log2 (ratio (siPKR HCV/siCt Mock)−(siCt HCV/siCt Mock) (indicated by log2*) with a cut-off of ≈2.0 fold.

doi:10.1371/journal.ppat.1002289.t001

pinpoint ISG15 as among the predictor genes of non-response to IFN therapy [14,15,16].

At present, we do not know at which level ISGylation regulates IFN induction in response to HCV infection. An HCV-mediated increase of ISG15 would favour preferential binding of ISG15 over that of ubiquitin to the E2 enzyme UbcH8 and hence enhance the spatio-temporal availability of UbcH8-ISG15 for HERC5 over that of UbcH8-ubiquitin for TRIM25. It may also lead to inhibition of TRIM25, through autoISGylation [21,34], which would decrease its ability to ubiquitinate RIG-I. We showed that overexpression of HERC5 together with Ube1L, UbcH8 and ISG15 was increasing the ability of ISG15 to inhibit IFN induction by HCV (**Figure 2B**). All three enzymes Ube1L, UbcH8 and HERC5 belong to the family of genes induced by IFN and it has been reported that ISGylation is optimum in a context of IFN treatment [18,35]. Therefore, it is tempting to speculate that elevated levels of ISG15 in some HCV-infected patients would bring the most favourable context for the virus when those patients are under IFN therapy. This would be in accord with the clinical data showing that HCV-induced high expression of ISG act as a negative predictive marker for response to IFN therapy.

It is doubtful that viruses with high IFN-inducing efficiency, such as Sendai virus may control RIG-I through ISG15 and PKR. However, viruses that avoid inducing IFN may have use of the PKR pathway. A good example might be that of Hepatitis B Virus (HBV) [36,37,38]. PKR expression was previously reported to be elevated in HCC liver from chronically HBV infected patients [39] and a relationship between PKR and IFN induction during HBV infection would be important to evaluate.

At present, we have established that HCV RNA interacts with PKR as soon as 2 hours post-infection. This interaction occurs prior the interaction of HCV RNA with RIG-I, which suggests that PKR may rapidly detect structures containing the incoming HCV RNA genome. Indeed, PKR has been reported to bind the dsRNA domains III and IV of HCV IRES [40] in addition to its ability to also bind 5′ triphosphorylated ss or dsRNA structures [41]. Whether PKR behaves as a pathogen recognition receptor for HCV RNA, like RIG-I, remains to be clarified. It is however clear that, in contrast to RIG-I, PKR acts here in favour of the pathogen rather than in favour of the host defense. We have established that the HCV RNA/PKR interaction depends on the first DRBD present at the N terminus of PKR and is independent on its kinase activity. The ability of PKR to serve as adapter in signaling pathways is not a total surprise since it has been previously shown to activate NF-κB through interaction of its C terminus with members of the TRAF family, such as TRAF5 and TRAF6 [42]. PKR contains also TRAF interacting motif in its N terminus [42] and an association between TRAF3 and PKR has been reported upon cotransfection in 293T cells [43]. Intriguingly, PKR was previously reported to participate in the induction of IFNβ, in association with MAVS, through activation of NF-κB or ATF-2 but not or partially IRF3; however these studies were not performed in the absence of RIG-I [44,45,46]. The mode of interaction between PKR, TRAF3 and MAVS, independently of RIG-I, and how it leads to a preferential induction of ISGs and not of IFNβ in response to HCV infection in contrast with the RIG-I/MAVS pathway remains to be determined. Based on our data, we propose now to divide the innate response to acute HCV infection into two phases: an early acute phase in which PKR is activated and a late acute phase that depends on RIG-I, the early phase controlling activation of the late phase. It is now essential to progress towards the generation of specific pharmaceutical inhibitors targeting PKR in order to abrogate the early acute phase to the benefit of the RIG-I-driven late phase. In a more general view, care should now be taken in the choice of compounds designed to be used as immune adjuvants, such as to be devoid of activation of the early acute PKR phase. This will ensure their efficiency as to activate properly the innate immune response through the late acute RIG-I phase.

Methods

Cell cultures and viruses

The culture of Huh7, Huh7.5, Huh7.25.CD81 cells, the preparation of Sendai virus stocks (≈2000 HAU/ml) and of HCV JFH1 stocks (≈6.10^4 FFU/mL and ≈6.10^6 FFU/mL) was as described [8,47]. Preparation and cultures of human primary hepatocytes was as described [48]. Of note, the ability of the Huh7.25.CD81 cells to induce IFN in response to SeV without prior IFN treatment (40-fold) was not observed in our previous study [8].The ability of Sendai virus to induce IFN is related to the presence of copyback DI (Defective Interfering) genomes [49]. The higher IFN inducing ability of the novel Sendai virus stock may have come from an important accumulation of these copyback DI genomes, during its growth in chicken eggs.

PKR inhibitors

The C16 compound [50] and the cell-permeable PRI peptide [51] were provided by Jacques Hugon. These drugs were applied (200 nM for C16 and 30 mM for PRI) one hour before the end of the 2 hr- incubation time with JFH1 and re-added to the medium after washing the cells with phosphate buffered saline (PBS). Note that PRI loses its effect very rapidly, probably through degradation in the cells, and requires to be added every hour to the cells until the end of treatment.

Expression vectors

TRIM25 was cloned from the IFN-treated Huh7.25CD81 cells (500 U/ml IFN-α2a; Cellsciences) after RT-PCR using the forward: 5′-ATGGCAGAGCTGTGCCCCCT-3′ and reverse 5′-CTACTTGGGGGAGCAGATGG-3′ primers. The pcDNA3.1(+) vector expressing 5′HA tagged-TRIM25 (provided by D. Garcin; University of Geneva, Switzerland) was used to generate the TRIM25 $P_{358}L$ construct by site-directed mutagenesis. The

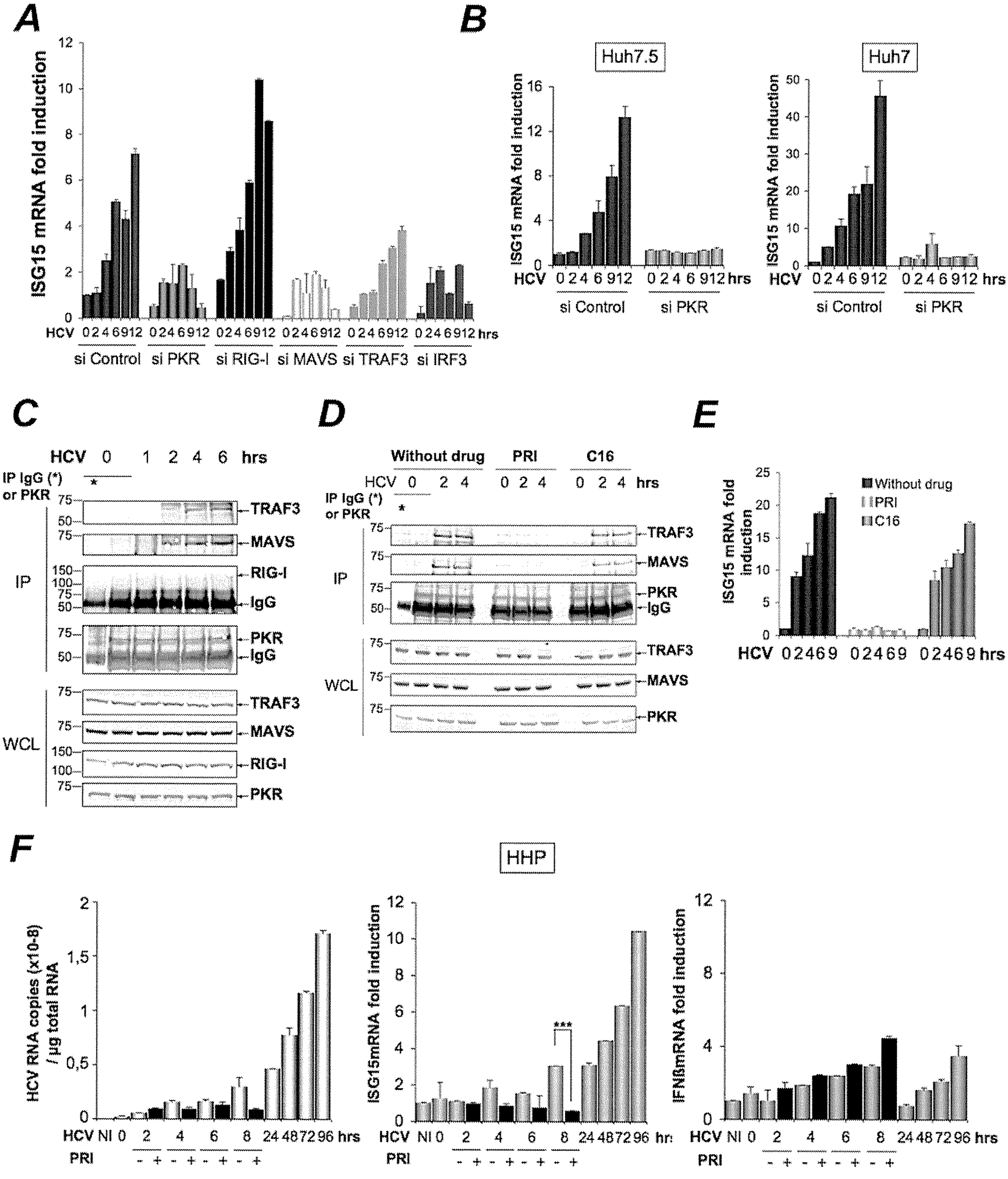

Figure 5. HCV-dependent induction of ISG15 involves PKR, MAVS and TRAF3 and not RIG-I. (**A–B**). **A**-The Huh7.25.CD81 cells were transfected with 50 nM Control siRNA and the different Smartpool siRNAs (50 nM siPKR; 10 nM siRIG-I; 5 nM siMAVS; 50 nM siTRAF3; 50 nM siIRF3) for 48 hrs and infected with JFH1 (m.o.i = 6). (**B**) Huh7.5 or Huh7 cells were transfected with siRNA Control or siPKR (50 nM) for 48 hrs and infected with JFH1 (m.o.i = 0.2 for Huh7.5 or 10 for Huh7). At the times indicated, expression of endogenous ISG15 was determined by RTqPCR and expressed as fold induction. Error bars represent the mean ±S.D for triplicates. The expression level of ISG15 RNA at the start of infection in the siControl cells was 9.97×10^4 copies (Huh7.25.CD81), 1.31×10^4 copies (Huh7.5) and 1.28×10^4 (Huh7). (**C–D**) Huh7.25.CD81 cells, in 100 cm^2 plates, were infected with JFH1 (m.o.i = 0.2) alone (**C**) or in presence of PRI or C16 (**D**). At the times indicated, cell extracts (3.5 mg) were processed for immunoprecipitation of PKR or for incubation with mouse IgG as a control of specificity (asterisk). The detection of the proteins in the complexes and in the whole cell extracts (WCE) was revealed by immunoblot using the Odyssey procedure. (**E**) The Huh7.25.CD81 cells were incubated with PRI or C16 and infected with JFH1 (m.o.i = 0.2) for the times indicated. Expression of endogenous ISG15 was determined as in A–B. The ISG15 RNA levels were 3.81×10^4 copies in the siControl cells. (**F**) Human primary hepatocytes (HHP) were infected with JFH1 (m.o.i = 6). One set of cells was incubated with 30 mM of the PRI inhibitor during 8 hours. At the times indicated, expression of HCV RNA, ISG15 and IFNβ was determined by RTqPCR. The expression levels of ISG15 and IFNβ RNA at the start of infection was 1.05×10^5 copies and $1,11\times10^4$ copies, respectively. Inhibition of induction of ISG15 by PRI at 8 hr post-infection was statistically significant (***; $p = 0.0001$).
doi:10.1371/journal.ppat.1002289.g005

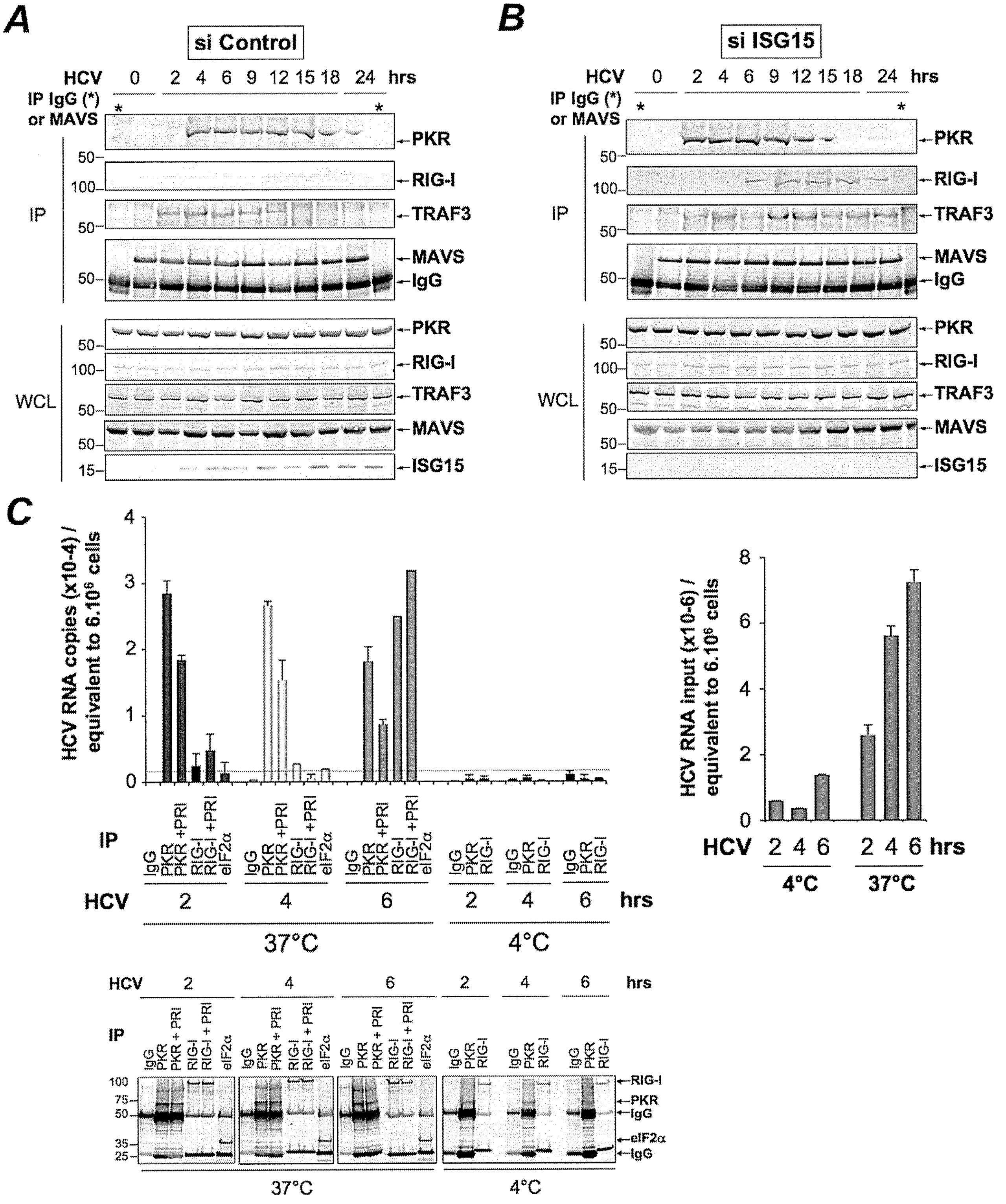

Figure 6. PKR both interacts with MAVS and TRAF3 and binds HCV RNA ahead of RIG-I. (**A–B**)- Huh7.25.CD81 cells were transfected with 25 nM of siRNA Control (**A**) or 25 nM of siRNA ISG15 (**B**) for 48 hrs and infected with JFH1 (m.o.i = 0.2). At the times indicated, cell extracts (4.5 mg) were incubated with anti-MAVS antibodies. In addition, cell extracts prepared at 0 hr post-infection were incubated with mouse IgG as a control of specificity (asterisk). The immunoprecipitated complexes were run on three different NuPAGE gels and blotted using Mab 71/10, anti-MAVS, anti-RIG-I or anti-TRAF3 antibodies. The expression level of each protein was controlled in the total cell extracts. (**C**)- Huh7.25.CD81 cells were incubated with JFH1 (m.o.i = 6) for 2 hrs at 37°C or at 4°C in the absence or presence of 30 μM of PRI. This drug was applied one hour before the end of the incubation time. After washing the cells twice with PBS, the cells were further incubated for 2, 4 or 6 hrs at 37°C or at 4°C in the absence or presence of PRI (added every hour). The cell extracts were processed for crosslinking of RNA to proteins before lysis, as described in Materials and Methods and different immunoprecipitations were performed with antibodies directed against PKR, RIG-I or eIF2α. After extensive washing, the presence of HCV RNA linked to the immunocomplexes was analysed by RTqPCR and the presence of the proteins was verified by Western blot. Measure of HCV RNA in

the cell extracts allowed to estimate its percentage of binding to PKR as 1.09%, 0.47% and 0.25% at 2, 4 and 6 hrs post-infection respectively, and its percentage of binding to RIG-I as 0.34% at 6 hrs post-infection.
doi:10.1371/journal.ppat.1002289.g006

IFNβ-firefly luciferase (pGL2-IFNβ) and pRL-TK Renilla-luciferase reporter plasmids were described previously [8]. The pGL3 luciferase reporter construct containing the −3 to −654 nucleotides of the ISG56 promoter was provided by N.Grandvaux [52]. The Myc-HIS-Ubiquitin construct was provided by R.Kopito (Stanford University, CA). ISG15 was cloned from IFN-treated Huh7 cells using the forward: 5′- GGATCCCATGGGCTGGGACCTGACGGTG-3′ and reverse 5′-CTCGAGCTCCGCCCGCCAGGCTCTGT-3′ primers and inserted into the pcDNA3.1(+)HA vector. The Ube1L, UbcH8 and HERC5 constructs were kindly provided by Jon M. Huibregtse [35]. The pcDNA1/AMP vector expressing PKR has been described previously [53].

RNA-mediated interference

The siRNAs directed against PKR, MAVS, RIG-I, TRAF3 and IRF3 which were used for the experiment described in figure 5A correspond to pools of siRNA (Smartpool) obtained from Dharmacon Research, Inc. (Lafayette, CO), as well as siRNAs directed against Ube1L used in Figure 2B. Control (scrambled) siRNA and siRNA directed against PKR or ISG15, used in all other experiments, were chemically synthesized by Dharmacon

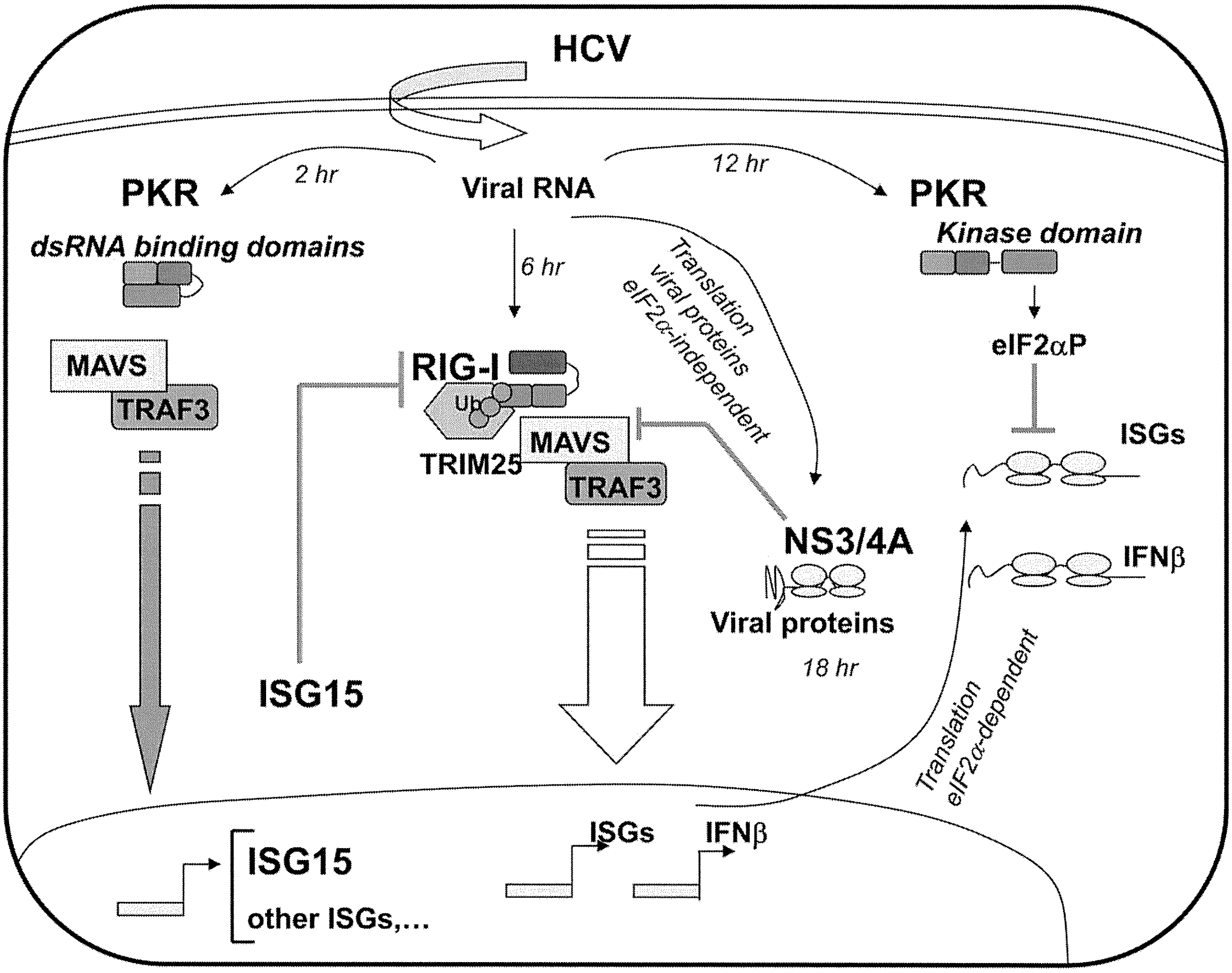

Figure 7. Multiple levels of control of IFN induction during HCV infection. Soon after infection, the HCV RNA is detected by the dsRNA binding domains (DRBD) of PKR ahead (2 hr) of its recognition by the RNA helicase RIG-I (6 hr). Recruitment of PKR by HCV triggers a signaling pathway that involves PKR as an adapter protein to recruit MAVS and TRAF3. This leads to a strong induction of the di-ubiquitine like protein ISG15 as well as other IRF3-dependent ISGs (Interferon-Stimulated Genes). ISG15 negatively controls the TRIM25-mediated ubiquitination (Ub) of RIG-I through an ISGylation process and thus interferes with the ability of RIG-I to recruit its downstream partners, including MAVS and TRAF3, and to induce IFNβ and ISGs. As the infection proceeds, HCV activates the eIF2α kinase function of PKR (12 hr). This leads to a transient (few hours) inhibition of general translation, including that of IFN [8] and ISGs [9] while the eIF2α-independent translation of the viral proteins proceeds unabated. At later times in the infection (18 hr), additional control of IFN induction occurs through cleavage of MAVS by the HCV NS3/4A protease, once the viral proteins have sufficiently accumulated in the cytosol [7,27].
doi:10.1371/journal.ppat.1002289.g007

(scrambled and PKR) and by EUROFINS MWG Operon (ISG15) (Text S1). The siRNAs (final concentration 25 nM or 50 nM) were transfected for 48 h using jetPRIME reagent according to the manufacturer's instructions (PolyPlus transfection TM) before transfection with other plasmids or before infection.

Antibodies

Mab to ISG15 (clone 2.1) was a kind gift of E.Borden [54]. Mab to PKR was produced from the murine 71/10 hybridoma (Agrobio; Fr) with kind permission of A.G.Hovanessian [55]. Other antibodies were as follows: anti-mouse IgG (Santa Cruz), anti-TRAF3 (Santa Cruz), pThr451-PKR (Alexis), MAVS (Alexis), anti-actin (Sigma), anti-pSer10-Histone H3 (Millipore), anti-HCV NS3 (Chemicon), anti-HCV core (Thermo scientific), anti-RIG-I (Alexis Biochemical Inc.), anti-TRIM25 (6105710; BD Bioscience), anti-IRF3 (Santa Cruz), anti-HA (12CA5; Roche) and anti-Myc (Santa Cruz).

Reporter assays

Huh7.25.CD81 cells (80,000 cells/well; 24-well plates) were transfected with 40 ng of pRL-TK Renilla-luciferase reporter (Promega) and 150 ng of either pGL2-IFNβ-Firefly luciferase reporter or pISG56-luciferase reporter and processed for dual-luciferase reporter assay as reported previously [8].

Real-time RT-PCR analysis

Total cellular RNA was extracted using the TRIZOL reagent (Invitrogen). HCV RNA was quantified by one-step RTqPCR. Reverse-transcription, amplification and real-time detection of PCR products were performed with 5 µl total RNA samples, using the SuperScript III Platinum one-step RTqPCR kit (Invitrogen) and an AbiPrism 7700 machine. For the sequence of the different primers, see Text S1. The results were normalized to the amount of cellular endogenous GAPDH RNA using the GAPDH control kit from EuroGentec. Copies number of HCV RNA may vary due to internal calibration and depending on the preparation of the viral stocks. All m.o.i were calculated using the titers expressed in FFU/ml. The IFNβ, ISG15, ISG56, Ube1L and GAPDH amplicons were quantified by a two-step RTqPCR assay as described [8].

Transcriptome analysis

Cellular RNA was extracted and purified from the cells using RNAeasy mini kit (QIAGEN K.K., Tokyo, Japan). Comprehensive DNA microarray analysis was performed with 3D-Gene Human Oligo chip25k with 2-color fluorescence method by New Frontiers Research Laboratories, Toray Industries Inc, Kamakura, Japan as previously described [56]. In brief, each sample was hybridized with 3D-Gene chip. Hybridization signals were scanned using Scan Array Express (PerkinElmer, Waltham, MA). The scanned image was analyzed using GenePix Pro (MDS Analytical Technologies, Sunnyvale, CA). All the analyzed data were scaled by global normalization.

Immunoprecipitation and immunoblot analysis

Cells were washed once with PBS and scraped into lysis buffer 1 (50 mM TRIS-HCl [pH 7.5], 140 mM NaCl, 5% glycerol, 1% CHAPS) that contained phosphatase and protease inhibitors (Complete, Roche Applied Science). The protein concentration was determined by the Bradford method. For immunoprecipitation, lysates were incubated at 4°C overnight with the primary antibodies as indicated and then in the presence of A/G-agarose beads (Santa Cruz Biotechnology) for 60 minutes. The beads were washed three times, and the precipitated proteins were extracted at 70°C using NuPAGE LDS sample buffer. Protein electrophoresis was performed on NuPAGE 4–12% Bis TRIS gels (Invitrogen). Proteins were transferred onto nitrocellulose membranes (Biorad), and probed with specific antibodies. Fluorescent immunoblot images were acquired and quantified by using an Odyssey scanner and the Odyssey 3.1 software (Li-Cor Biosciences) as described previously [8]. For detection of ISG15, cells were lysed in RIPA buffer (50 mM TRIS-HCl [pH 8.0]; 200 mM NaCl; 1% NP-40; 0.5% Sodium Deoxycholate; 0.05% SDS; 2 mM EDTA) and protein electrophoresis was performed on 4–20% polyacrylamide gels (PIERCE).

Nuclear/cytoplasmic extract

Pellets from cells washed in ice-cold phosphate-buffered saline (PBS) were lysed in ice-cold cytoplasmic buffer (10 mM TRIS [pH 8.0], 5 mM EDTA, 0.5 mM EGTA, 0.25% Triton X-100) containing phosphatase and protease inhibitors. The suspension was centrifuged for 30 seconds at 14,000 g and the supernatant (cytoplasmic fraction) was transferred into microcentrifuge tubes. The nuclear pellet was resuspended in Urea buffer (8 M Urea, 10 mM TRIS [pH 7,4], 1 mM EDTA, 1 mM dithiothreitol) containing phosphatase and protease inhibitors, homogenized by vortex and boiled for 10 minutes. The protein concentration was determined by the Bradford method.

Ubiquitination assay

Huh7.25.CD81 cells were transfected for 48 hrs with 5 µg of Myc-His-Ubiquitin expression plasmid using jetPRIME reagent. The cells were then washed in ice-cold PBS containing 20 mM N-ethylmaleimide (Sigma-Aldrich), harvested directly in Gua8 buffer (6 M guanidine-HCl, 300 mM NaCl, 50 mM Na_2HPO_4, 50 mM NaH_2PO_4 [pH 8.0]), briefly sonicated, and centrifuged at 14,000 g for 15 min at 4°C. 1/10th of the lysate was subjected to precipitation with 10% trichloroacetic acid for protein analysis in whole cell extracts. The rest of the lysate was incubated for 2 hrs with 20 µl (packed volume) of Talon resin Ni-affinity beads (Clontech) on a rotating wheel. Bound proteins were washed four times in Gua8 buffer, three times in Urea 6.3 buffer (8 M Urea, 10 mM TRIS, 0.1 M Na_2HPO_4, 20 mM Imidazole [pH 6.3]), and three times in cold PBS, after which they were eluted by boiling in NuPAGE LDS sample buffer. Electrophoresis was performed on 4–12% of acrylamide NuPAGE gels (Invitrogen).

Co-precipitation protein/HCV RNA

Huh7.25.CD81 cells were incubated for 10 min in their culture medium containing 1/10 volume (Vol) of a crosslinking solution (11% Formaldehyde, 0.1 M NaCl, 1 mM Na-EDTA-[pH 8], 0.5 mM Na-EGTA-[pH 8], 50 mM HEPES [pH 8]). The reaction was stopped by addition of a solution of 0.125 M glycine in PBS [pH 8] at room temperature (RT). The cells were washed three times in ice-cold PBS containing 1000 U/ml of RNAse inhibitor (Promega), scraped in PBS and dispatched into three sets containing ½ (set 1), ¼ (set 2) and ¼ (set 3) of the cell suspension. The three sets were centrifuged for 30 seconds at 14,000 g and 4°C and the cell pellets were lysed into lysis buffer 1 containing phosphatase/protease and RNAse inhibitors (Promega) for sets 1 and 2 or into TRIZOL reagent for set 3. Cell lysates from sets 1 and 2 were then incubated at 4°C, first overnight with the appropriate primary antibodies and for 60 minutes in the presence of A/G-agarose beads (Santa Cruz Biotechnology). After the incubation period, the beads were washed four times with buffer 1. Set 1 (HCV RNA bound to immunocomplexes) and set 3 (input HCV RNA) were submitted to TRIZOL treatment and HCV

RNA was quantified by one-step RTqPCR as described previously. The immunoprecipitated proteins from set 2 were extracted at 70°C using NuPAGE LDS sample buffer and analysed by immunoblot after electrophoresis on 4–12% of acrylamide NuPAGE gels (Invitrogen).

Supporting Information

Figure S1 Efficient induction of TRIM25 by IFN in the Huh7.25.CD81 cells. Huh7.25.CD81 cells, seeded at 8×10^4 cells in 24-well plates containing coverslips, were treated with 500 U/ml of IFNα for 24 hrs (IFN) or left untreated (Cont). Cells were fixed with 4% PFA and TRIM25 was detected using anti-TRIM25 antibodies (red). Nuclei are shown in blue after DAPI labelling. Microscope magnification was ×63.
(PDF)

Figure S2 HCV controls RIG-I ubiquitination through ISG15 in the Huh7 cells. Huh7 cells were transfected for 24 hrs with 25 nM of siRNA (Control or ISG15) and for another 24 hr with 5 µg of a His-Myc-Ubiquitin plasmid in absence or presence of 5 µg of a plasmid expressing HA-TRIM25. The cells were infected with JFH1 (m.o.i = 0.2). At the times indicated, cell extracts were processed for analysis of RIG-I ubiquitination and the expression of the different proteins in the total cell extracts. Efficiency of infection by JFH1 in the Huh7 cells was 2 log less than in the Huh7.25.CD81 cells.
(PDF)

Figure S3 Expression of ISG15 and ISG15 conjugating enzymes inhibit IFN induction in response to SeV. Huh7.25.CD81 cells were transfected with a plasmid expressing HA-ISG15 alone or in the presence of plasmids expressing the ISG15 conjugating enzymes Ube1L (E1), UbcH8 (E2) and HERC5 (E3). The cells were then infected with JFH1 (m.o.i = 6) for the times indicated. Stimulation of endogenous IFNβ RNA expression was determined by RTqPCR and expressed as fold induction. The degree of statistical significance is indicated by stars after calculation of the p-values (from left to right: 0.0124 and 0.0058).
(PDF)

Figure S4 Control of efficiency of siRNA Ube1L in the Huh7.25.CD81 cells. The Huh7.25.CD81 cells were transfected with 50 nM of siRNA directed against Ube1L for 48 hours and infected with HCV. RNA was prepared from the cells at different times post infection as indicated and expression levels of Ube1L was determined by RTqPCR.
(PDF)

Figure S5 Modulation of PKR activation by ISG15. Huh7.25.CD81 cells, in 100 cm^2 plates, were transfected with siRNA Control or siRNA ISG15 or transfected with a plasmid expressing HA-ISG15 for 48 hrs and infected with JFH1 (m.o.i = 6). At the indicated times post-infection, cell extracts (2.2 mg) were processed for immunoprecipitation of PKR. The immunoprecipitated complexes were run on two different NuPAGE gels and blotted using Mab 71/10 or anti-phosphorylated PKR antibodies (PKR-P). The presence of PKR and PKR-P was revealed using the Odyssey procedure. The bands corresponding to total PKR and phosphorylated PKR were quantified using the Odyssey software and expressed as the ratio PKR-P/PKR in the absence (siISG15) and in the presence of ISG15 in the control cells (Control) or after transfection of the ISG15 expressing plasmid (HA-ISG15).
(PDF)

Figure S6 Induction of ISG56 by Sendai virus in the Huh7.25.CD81 cells does not depend on PKR. Huh7.25.CD81 cells were either transfected with 25 nM of siRNA Control or 25 nM siPKR for 24 hrs and infected with SeV for the times indicated. The effect of PKR silencing on the stimulation of expression of endogenous ISG56 was determined by RTqPCR and expressed as fold induction. Error bars represent the mean ±S.D for triplicates. The expression levels of ISG56 RNA at the start of infection were respectively 1.15×10^5 copies (siControl) and 1.16×10^5 copies (siPKR).
(PDF)

Figure S7 Control of the efficiency of siRNA treatment in the Huh7.25.CD81 cells. The Huh7.25.CD81 cells were transfected for 48 hrs with 50 nM Control siRNA or with the different Smartpool siRNAs as shown (50 nM siPKR; 10 nM siRIG-I; 50 nM siIRF3; 50 nM siTRAF3; 5 nM siMAVS). Total cell extracts were prepared and the expression level of each protein, as well as that of actin used as control, was revealed by immunoblot and Odyssey procedure after a run on NuPAGE gels. Under each lane, the numbers represent the quantification of the different protein bands performed using the Odyssey software.
(TIF)

Figure S8 HCV triggers nuclear translocation of IRF3 early after infection in the Huh7.25.CD81 cells. Huh7.25.CD81 cells, seeded at 10^5 cells in 24-well plates containing coverslips, were infected for different times (0, 4 and 6 hours) at 37°C with JFH1 (moi = 6) or with SeV (40 HAU/ml) in the absence or in the presence of 10 ng/ml Leptomycine B (LB; Sigma), which was used here as a convenient mean to enhance the nuclear detection of IRF3 since it can interfere with nuclear export [57]. Cells were fixed with 4% PFA and IRF3 was detected using anti-IRF3 antibodies (red). Nuclei are shown in blue after DAPI labelling. The arrows show the presence of IRF3 in the nucleus. Microscope magnification was ×63.
(PDF)

Figure S9 Induction of ISG56 by HCV in the Huh7.5 and Huh7 cells depends on PKR. Huh7.5 or Huh7 cells were transfected with siRNA Control or siPKR (50 nM) for 48 hrs and infected with JFH1 (m.o.i = 0.2 for Huh7.5 or 10 for Huh7). At the times indicated, expression of endogenous ISG56 was determined by RTqPCR and expressed as fold induction. Error bars represent the mean ±S.D for triplicates. The expression levels of ISG56 RNA at the start of infection in the siControl cells was 1.37×10^4 copies (Huh7.5 cells) and 1.28×10^4 copies (Huh7 cells).
(PDF)

Figure S10 Induction of ISG56 by HCV is specifically inhibed by the PKR inhibitor PRI. The Huh7.25.CD81 cells were incubated with PRI or C16 and infected with JFH1 (m.o.i = 0.2) for the times indicated. RTqPCR analysis of endogenous ISG56 was determined by RTqPCR and expressed as fold induction. The expression levels of ISG56 RNA at the start of infection in the control cells was 1.97×10^4 copies.
(TIF)

Figure S11 The RNAse inhibitor RNAsin does not favour the formation of a RIG-I/PKR complex upon HCV infection. Two sets of Huh7.25.CD81 cells were plated into 100 cm^2 plates and infected with JFH1. At the times indicated, cell extracts (3.5 mg) from the two sets were processed similarly for immunoprecipitation of PKR or for incubation with mouse IgG as a control of specificity (asterisk), except that care was taken to add the RNAse inhibitor RNAsin (1000 U/ml) at all steps for the second set (+RNAsin). Detection of RIG-I, MAVS, and PKR in

the complexes and in the whole cell extracts (WCE) was revealed by immunoblot using the Odyssey procedure. Detection of Actin in WCE served as loading control.
(PDF)

Table S1 Transcriptome analysis of PKR-dependent downpregulated gene upon 12 hrs of HCV infection. Preparation of samples was as described under Table 1. The list shows genes that were affected no more than twice by the depletion of PKR in the control cells (0.5< siPKR mock/siCt <1.6). The dependence of each of these genes in regards with PKR for their inhibition by HCV is expressed as log2 (ratio (siPKR HCV/siCt Mock)−(siCt HCV/siCt Mock) (indicated by log2*) with a cut-off of ≈2.0 fold.
(DOC)

Text S1 Supplementary methods.
(DOC)

Acknowledgments

We thank Michael Gale Jr, Pierre-Olivier Vidalain and Christine Neuveut for critical reviews of the manuscript. We thank Adrien Six, Eric Batsche and Agata Budkowska for discussions. We thank Ernest Borden for the gift of anti-ISG15 antibodies, Jon Huibregste for the gift of plasmids expressing ISG15 conjugating enzymes, Dominique Garcin for providing the Sendai virus, Claire Gondeau and Martine Daujat for their help in the preparation and infection of human primary hepatocytes with JFH1.

Author Contributions

Conceived and designed the experiments: NA TW EFM. Performed the experiments: NA SD DA MF FS-O. Analyzed the data: NA TW EFM. Contributed reagents/materials/analysis tools: JH DA MF FS-O TW. Wrote the paper: NA EFM.

References

1. Gack MU, Shin YC, Joo CH, Urano T, Liang C, et al. (2007) TRIM25 RING-finger E3 ubiquitin ligase is essential for RIG-I-mediated antiviral activity. Nature 446: 916–920.
2. Gack MU, Kirchhofer A, Shin YC, Inn KS, Liang C, et al. (2008) Roles of RIG-I N-terminal tandem CARD and splice variant in TRIM25-mediated antiviral signal transduction. Proc Natl Acad Sci U S A 105: 16743–16748.
3. Yoneyama M, Fujita T (2009) RNA recognition and signal transduction by RIG-I-like receptors. Immunol Rev 227: 54–65.
4. Binder M, Kochs G, Bartenschlager R, Lohmann V (2007) Hepatitis C virus escape from the interferon regulatory factor 3 pathway by a passive and active evasion strategy. Hepatology 46: 1365–1374.
5. Saito T, Owen DM, Jiang F, Marcotrigiano J, Gale M, Jr. (2008) Innate immunity induced by composition-dependent RIG-I recognition of hepatitis C virus RNA. Nature 454: 523–527.
6. Sumpter R, Jr., Loo YM, Foy E, Li K, Yoneyama M, et al. (2005) Regulating intracellular antiviral defense and permissiveness to hepatitis C virus RNA replication through a cellular RNA helicase, RIG-I. J Virol 79: 2689–2699.
7. Meylan E, Curran J, Hofmann K, Moradpour D, Binder M, et al. (2005) Cardif is an adaptor protein in the RIG-I antiviral pathway and is targeted by hepatitis C virus. Nature 437: 1167–1172.
8. Arnaud N, Dabo S, Maillard P, Budkowska A, Kalliampakou KI, et al. (2010) Hepatitis C virus controls interferon production through PKR activation. PLoS One 5: e10575.
9. Garaigorta U, Chisari FV (2009) Hepatitis C virus blocks interferon effector function by inducing protein kinase R phosphorylation. Cell Host Microbe 6: 513–522.
10. Mihm S, Frese M, Meier V, Wietzke-Braun P, Scharf JG, et al. (2004) Interferon type I gene expression in chronic hepatitis C. Lab Invest 84: 1148–1159.
11. Sarasin-Filipowicz M, Oakeley EJ, Duong FH, Christen V, Terracciano L, et al. (2008) Interferon signaling and treatment outcome in chronic hepatitis C. Proc Natl Acad Sci U S A 105: 7034–7039.
12. Bigger CB, Guerra B, Brasky KM, Hubbard G, Beard MR, et al. (2004) Intrahepatic gene expression during chronic hepatitis C virus infection in chimpanzees. J Virol 78: 13779–13792.
13. Takahashi K, Asabe S, Wieland S, Garaigorta U, Gastaminza P, et al. (2010) Plasmacytoid dendritic cells sense hepatitis C virus-infected cells, produce interferon, and inhibit infection. Proc Natl Acad Sci U S A 107: 7431–7436.
14. Askarieh G, Alsio A, Pugnale P, Negro F, Ferrari C, et al. (2010) Systemic and intrahepatic interferon-gamma-inducible protein 10 kDa predicts the first-phase decline in hepatitis C virus RNA and overall viral response to therapy in chronic hepatitis C. Hepatology 51: 1523–1530.
15. Asselah T, Bieche I, Narguet S, Sabbagh A, Laurendeau I, et al. (2008) Liver gene expression signature to predict response to pegylated interferon plus ribavirin combination therapy in patients with chronic hepatitis C. Gut 57: 516–524.
16. Chen L, Borozan I, Feld J, Sun J, Tannis LL, et al. (2005) Hepatic gene expression discriminates responders and nonresponders in treatment of chronic hepatitis C viral infection. Gastroenterology 128: 1437–1444.
17. Chen L, Sun J, Meng L, Heathcote J, Edwards A, et al. (2010) ISG15, a ubiquitin-like interferon stimulated gene, promotes Hepatitis C Virus production in vitro: Implications for chronic infection and response to treatment. J Gen Virol 91: 382–388.
18. Kim MJ, Hwang SY, Imaizumi T, Yoo JY (2008) Negative feedback regulation of RIG-I-mediated antiviral signaling by interferon-induced ISG15 conjugation. J Virol 82: 1474–1483.
19. Akazawa D, Date T, Morikawa K, Murayama A, Miyamoto M, et al. (2007) CD81 expression is important for the permissiveness of Huh7 cell clones for heterogeneous hepatitis C virus infection. J Virol 81: 5036–5045.
20. Nisole S, Stoye JP, Saib A (2005) TRIM family proteins: retroviral restriction and antiviral defence. Nat Rev Microbiol 3: 799–808.
21. Zou W, Wang J, Zhang DE (2007) Negative regulation of ISG15 E3 ligase EFP through its autoISGylation. Biochem Biophys Res Commun 354: 321–327.
22. Jeon YJ, Yoo HM, Chung CH (2010) ISG15 and immune diseases. Biochim Biophys Acta 1802: 485–496.
23. Kim KI, Yan M, Malakhova O, Luo JK, Shen MF, et al. (2006) Ube1L and protein ISGylation are not essential for alpha/beta interferon signaling. Mol Cell Biol 26: 472–479.
24. Chen WH, Basu S, Bhattacharjee AK, Cross AS (2010) Enhanced antibody responses to a detoxified lipopolysaccharide-group B meningococcal outer membrane protein vaccine are due to synergistic engagement of Toll-like receptors. Innate Immun 16: 322–332.
25. Broering R, Zhang X, Kottilil S, Trippler M, Jiang M, et al. (2010) The interferon stimulated gene 15 functions as a proviral factor for the hepatitis C virus and as a regulator of the IFN response. Gut 59: 1111–1119.
26. Elco CP, Guenther JM, Williams BRG, Sen GC (2005) Analysis of genes induced by Sendai virus infection of mutant cell lines reveals essential roles of interferon regulatory factor 3, NF-kappaB, and interferon but not toll-like receptor 3. J Virol 79: 3920–3929.
27. Loo YM, Owen DM, Li K, Erickson AK, Johnson CL, et al. (2006) Viral and therapeutic control of IFN-beta promoter stimulator 1 during hepatitis C virus infection. Proc Natl Acad Sci U S A 103: 6001–6006.
28. Bigger CB, Brasky KM, Lanford RE (2001) DNA microarray analysis of chimpanzee liver during acute resolving hepatitis C virus infection. J Virol 75: 7059–7066.
29. Farell PJ, Broeze RJ, Lengyel P (1979) Accumulation of an mRNA and protein in interferon-treated Ehrlich ascites tumour cells. Nature (London) 279: 523–524.
30. Haas AL, Ahrens P, Bright PM, Ankel H (1987) Interferon induces a 15-kilodalton protein exhibiting marked homology to ubiquitin. J Biol Chem 262: 11315–11323.
31. Zhao C, Denison C, Huibregtse JM, Gygi S, Krug RM (2005) Human ISG15 conjugation targets both IFN-induced and constitutively expressed proteins functioning in diverse cellular pathways. Proc Natl Acad Sci U S A 102: 10200–10205.
32. Yuan W, Krug RM (2001) Influenza B virus NS1 protein inhibits conjugation of the interferon (IFN)-induced ubiquitin-like ISG15 protein. Embo J 20: 362–371.
33. Wong JJ, Pung YF, Sze NS, Chin KC (2006) HERC5 is an IFN-induced HECT-type E3 protein ligase that mediates type I IFN-induced ISGylation of protein targets. Proc Natl Acad Sci U S A 103: 10735–10740.
34. Zou W, Zhang DE (2006) The interferon-inducible ubiquitin-protein isopeptide ligase (E3) EFP also functions as an ISG15 E3 ligase. J Biol Chem 281: 3989–3994.
35. Durfee LA, Lyon N, Seo K, Huibregtse JM (2010) The ISG15 conjugation system broadly targets newly synthesized proteins: implications for the antiviral function of ISG15. Mol Cell 38: 722–732.
36. Wieland SF, Chisari FV (2005) Stealth and cunning: hepatitis B and hepatitis C viruses. J Virol 79: 9369–9380.
37. Jiang J, Tang H (2010) Mechanism of inhibiting type I interferon induction by hepatitis B virus×protein. Prein Cell 1: 1106–1117.
38. Wei C, Ni C, Song T, Liu Y, Yang X, et al. (2010) The hepatitis B virus×protein disrupts innate immunity by downregulating mitochondrial antiviral signaling protein. J Immunol 185: 1158–1168.
39. Chen GG, Lai PB, Ho RL, Chan PK, Xu H, et al. (2004) Reduction of double-stranded RNA-activated protein kinase in hepatocellular carcinoma associated with hepatitis B virus. J Med Virol 73: 187–194.

40. Shimoike T, McKenna SA, Lindhout DA, Puglisi JD (2009) Translational insensitivity to potent activation of PKR by HCV IRES RNA. Antiviral Res 83: 228–237.
41. Nallagatla SR, Hwang J, Toroney R, Zheng X, Cameron CE, et al. (2007) 5′-triphosphate-dependent activation of PKR by RNAs with short stem-loops. Science 318: 1455–1458.
42. Gil J, Garcia MA, Gomez-Puertas P, Guerra S, Rullas J, et al. (2004) TRAF family proteins link PKR with NF-kappa B activation. Mol Cell Biol 24: 4502–4512.
43. Oganesyan G, Saha SK, Guo B, He JQ, Shahangian A, et al. (2006) Critical role of TRAF3 in the Toll-like receptor-dependent and -independent antiviral response. Nature 439: 208–211.
44. Zhang P, Samuel CE (2008) Induction of protein kinase PKR-dependent activation of interferon regulatory factor 3 by vaccinia virus occurs through adapter IPS-1 signaling. J Biol Chem 283: 34580–34587.
45. McAllister CS, Samuel CE (2009) The RNA-activated protein kinase enhances the induction of interferon-beta and apoptosis mediated by cytoplasmic RNA sensors. J Biol Chem 284: 1644–1651.
46. McAllister CS, Toth AM, Zhang P, Devaux P, Cattaneo R, et al. (2010) Mechanisms of protein kinase PKR-mediated amplification of beta interferon induction by C protein-deficient measles virus. J Virol 84: 380–386.
47. Strahle L, Marq JB, Brini A, Hausmann S, Kolakofsky D, et al. (2007) Activation of the beta interferon promoter by unnatural Sendai virus infection requires RIG-I and is inhibited by viral C proteins. J Virol 81: 12227–12237.
48. Biron-Andreani C, Raulet E, Pichard-Garcia L, Maurel P (2010) Use of human hepatocytes to investigate blood coagulation factor. Methods Mol Biol 640: 431–445.
49. Strahle L, Garcin D, Kolakofsky D (2006) Sendai virus defective-interfering genomes and the activation of interferon-beta. Virology 351: 101–111.
50. Jammi NV, Whitby LR, Beal PA (2003) Small molecule inhibitors of the RNA-dependent protein kinase. Biochem Biophys Res Commun 308: 50–57.
51. Nekhai S, Bottaro DP, Woldehawariat G, Spellerberg A, Petryshyn R (2000) A cell-permeable peptide inhibits activation of PKR and enhances cell proliferation. Peptides 21: 1449–1456.
52. Grandvaux N, Servant MJ, tenOever B, Sen GC, Balachandran S, et al. (2002) Transcriptional profiling of interferon regulatory factor 3 target genes: direct involvement in the regulation of interferon-stimulated genes. J Virol 76: 5532–5539.
53. Bonnet MC, Daurat C, Ottone C, Meurs EF (2006) The N-terminus of PKR is responsible for the activation of the NF-kappaB signaling pathway by interacting with the IKK complex. Cell Signal 18: 1865–1875.
54. Malakhov MP, Kim KI, Malakhova OA, Jacobs BS, Borden EC, et al. (2003) High-throughput immunoblotting. Ubiquitiin-like protein ISG15 modifies key regulators of signal transduction. J Biol Chem 278: 16608–16613.
55. Laurent AG, Krust B, Galabru J, Svab J, Hovanessian AG (1985) Monoclonal antibodies to interferon induced 68,000 Mr protein and their use for the detection of double-stranded RNA dependent protein kinase in human cells. Proc Natl Acad SciUSA 82: 4341–4345.
56. Iwano S, Ichikawa M, Takizawa S, Hashimoto H, Miyamoto Y (2010) Identification of AhR-regulated genes involved in PAH-induced immunotoxicity using a highly-sensitive DNA chip, 3D-Gene Human Immunity and Metabolic Syndrome 9k. Toxicol In Vitro 24: 85–91.
57. Wolff B, Sanglier JJ, Wang Y (1997) Leptomycin B is an inhibitor of nuclear export: inhibition of nucleo-cytoplasmic translocation of the human immunodeficiency virus type 1 (HIV-1) Rev protein and Rev-dependent mRNA. Chem Biol 4: 139–147.

Delayed-Onset Caspase-Dependent Massive Hepatocyte Apoptosis upon Fas Activation in Bak/Bax-Deficient Mice

Hayato Hikita,[1]* Tetsuo Takehara,[1]* Takahiro Kodama,[1] Satoshi Shimizu,[1] Minoru Shigekawa,[1] Atsushi Hosui,[1]
Takuya Miyagi,[1] Tomohide Tatsumi,[1] Hisashi Ishida,[1] Wei Li,[1] Tatsuya Kanto,[1] Naoki Hiramatsu,[1]
Shigeomi Shimizu,[2] Yoshihide Tsujimoto,[3] and Norio Hayashi[4]

The proapoptotic Bcl-2 family proteins Bak and Bax serve as an essential gateway to the mitochondrial pathway of apoptosis. When activated by BH3-only proteins, Bak/Bax triggers mitochondrial outer membrane permeabilization leading to release of cytochrome c followed by activation of initiator and then effector caspases to dismantle the cells. Hepatocytes are generally considered to be type II cells because, upon Fas stimulation, they are reported to require the BH3-only protein Bid to undergo apoptosis. However, the significance of Bak and Bax in the liver is unclear. To address this issue, we generated hepatocyte-specific Bak/Bax double knockout mice and administered Jo2 agonistic anti-Fas antibody or recombinant Fas ligand to them. Fas-induced rapid fulminant hepatocyte apoptosis was partially ameliorated in Bak knockout mice but not in Bax knockout mice, and was completely abolished in double knockout mice 3 hours after Jo2 injection. Importantly, at 6 hours, double knockout mice displayed severe liver injury associated with repression of XIAP, activation of caspase-3/7 and oligonucleosomal DNA breaks in the liver, without evidence of mitochondrial disruption or cytochrome c–dependent caspase-9 activation. This liver injury was not ameliorated in a cyclophilin D knockout background nor by administration of necrostatin-1, but was completely inhibited by administration of a caspase inhibitor after Bid cleavage. Conclusion: Whereas either Bak or Bax is critically required for rapid execution of Fas-mediated massive apoptosis in the liver, delayed onset of mitochondria-independent, caspase-dependent apoptosis develops even in the absence of both. The present study unveils an extrinsic pathway of apoptosis, like that in type I cells, which serves as a backup system even in type II cells. (HEPATOLOGY 2011;54:240-251)

See Editorial on Page 13

Fas, also called APO-1 and CD95, is one of the death receptors that are potent inducers of apoptosis and constitutively expressed by every cell type in the liver.[1] Dysregulation of Fas-mediated apoptosis is involved in several liver diseases.[2] In the liver of patients with chronic hepatitis C, Fas is overexpressed in correlation with the degree of hepatitis, and Fas ligand can be detected in liver-infiltrating mononuclear cells.[3,4] Fas is also strongly expressed in the livers of patients with chronic hepatitis B, autoimmune hepatitis, and nonalcoholic steatohepatitis.[4,5] Moreover, in the liver of patients with fulminant hepatitis, Fas is up-regulated with strong detection of Fas ligand.[6] In mice, injection of Jo2 agonistic anti-Fas antibody leads

---

Abbreviations: ALT, alanine aminotransferase; CypD, cyclophilin D; DISC, death-inducing signaling complex; DKO, double knockout; DMSO, dimethylsulfoxide; IAP, inhibition of apoptosis protein; KO, knockout; PARP, poly(adenosine diphosphate ribose) polymerase; RIP, receptor-interacting protein; TUNEL, terminal deoxynucleotidyl transferase–mediated deoxyuridine triphosphate nick-end labeling; WT, wild-type.

From the [1]Departments of Gastroenterology and Hepatology; and [3]Molecular Genetics, Osaka University Graduate School of Medicine, Suita, Osaka, Japan; the [2]Department of Pathological Cell Biology, Medical Research Institute, Tokyo Medical and Dental University, Bunkyo-ku, Tokyo, Japan; and [4]Kansai-Rosai Hospital, Amagasaki, Hyogo, Japan.

Received December 27, 2010; accepted March 9, 2011.

Supported in part by a Grant-in-Aid for Scientific Research from the Ministry of Education, Culture, Sports, Science, and Technology (to T. Takehara) and a Grant-in-Aid for Research on Hepatitis from the Ministry of Health, Labour, and Welfare of Japan.

**These authors contributed equally to this work.*

to massive hepatocyte apoptosis and lethality, suggesting that the hepatocyte is one of the most sensitive cell types to Fas stimulation.[7] This model is considered to at least partly mimic human fulminant liver failure.

Fas, upon ligation by Fas ligand, activates caspase-8 through the recruitment of Fas-associated protein with a death domain and formation of the death-inducing signaling complex (DISC).[1,2] Whereas activated caspase-8 directly activates effector caspases such as caspase-3 and caspase-7 through the so-called extrinsic pathway, leading to apoptosis in type I cells, it activates caspase-3/7 through the mitochondrial pathway in type II cells. In type II cells, activated caspase-8 cleaves the BH3-only protein Bid into its truncated form, which in turn directly or indirectly activates and homo-oligomerizes Bak and/or Bax to form pores at the mitochondrial outer membrane, leading to the release of cytochrome c. After being released, cytochrome c assembles with Apaf-1 to form apoptosomes which promote self-cleavage of procaspase-9 followed by activation of caspase-3/7 to cleave a variety of cellular substrates such as poly(adenosine diphosphate ribose) polymerase (PARP) and finally to execute apoptosis.[8,9] Hepatocytes are considered to be typical type II cells, because Bid knockout (KO) mice were reported to be resistant to hepatocyte apoptosis upon Fas activation.[10,11] Although Bak and Bax are crucial gateways to apoptosis of the mitochondrial pathway, little information is available about their significance in hepatocyte apoptosis because most traditional Bak/Bax double knockout (DKO) mice ($bak^{-/-}$ $bax^{-/-}$) die perinatally.[12]

In the present study, we tried to address this issue by generating hepatocyte-specific Bak/Bax DKO mice. We demonstrate that either Bak or Bax is required and sufficient to induce Fas-mediated early-onset hepatocyte apoptosis and lethal liver injury. Importantly, even if deficient in both Bak and Bax, Bak/Bax DKO mice still develop delayed-onset caspase-dependent massive hepatocyte apoptosis, suggesting that the mitochondria-independent pathway of apoptosis, as observed in type I cells, works as a backup system when the mitochondrial pathway of apoptosis in the liver is absent. This study is the first to demonstrate the significant but limited role of Bak and Bax in executing Fas-induced apoptosis in the liver.

Materials and Methods

Mice. Heterozygous Alb-Cre transgenic mice expressing Cre recombinase gene under the promoter of the albumin gene were described.[13] We purchased Bak KO mice ($bak^{-/-}$), Bax KO mice ($bax^{-/-}$), and Bak KO mice carrying the *bax* gene flanked by 2 *lox*P sites ($bak^{-/-}$ $bax^{flox/flox}$) from the Jackson Laboratory (Bar Harbor, ME). Traditional cyclophilin D (CypD) KO mice have been described.[14] All mice strains that we used were created from a mixed background (C57BL/6 and 129). We generated hepatocyte-specific Bak/Bax DKO mice ($bak^{-/-}$ $bax^{flox/flox}$ *Alb-Cre*) or hepatocyte-specific CypD/Bak/Bax triple KO mice ($cypd^{-/-}$ $bak^{-/-}$ $bax^{flox/flox}$ *Alb-Cre*) by mating the strains. Mice were injected intraperitoneally with 1.5 or 0.5 mg/kg Jo2 anti-Fas antibody (BD Bioscience, Franklin Lakes, NJ) or intravenously with 0.25 mg/kg recombinant Fas ligand (Alexis Biochemicals, San Diego, CA) cross-linked with 0.5 mg/kg anti-Flag M2 antibody (Sigma-Aldrich, St. Louis, MO) to induce apoptosis. In some experiments, mice were intraperitoneally injected with 2 mg/kg necrostatin-1 (Sigma-Aldrich) or 40 mg/kg Q-VD-Oph (R&D Systems, Minneapolis, MN). They were maintained in a specific pathogen-free facility and treated with humane care with approval from the Animal Care and Use Committee of Osaka University Medical School.

Apoptosis Assay. Measurement of serum alanine aminotransferase (ALT) levels, hematoxylin and eosin staining, and terminal deoxynucleotidyl transferase–mediated deoxyuridine triphosphate nick-end labeling (TUNEL) of liver sections have been described.[15] Analysis of cytochrome c release from isolated mitochondria have also been described.[16] To detect DNA fragmentation, 1.5 μg DNA extracted from 30 mg liver tissue by Maxwell16 (Promega, Madison, WI) was incubated with 0.5 μg RNase A (Qiagen, Tokyo, Japan) and separated by way of electrophoresis on a 1.5% agarose gel.

Western Blot Analysis. For western immunoblotting, the following antibodies were used: anti–full-length Bid, anti–Cox IV, anti–cleaved caspase-3, anti–caspase-7, anti–caspase-8, anti–caspase-9, anti-PARP, anti-Bax, anti-cIAP1, and anti-XIAP antibodies were

---

Address reprint requests to: Tetsuo Takehara, M.D., Ph.D., Department of Gastroenterology and Hepatology, Osaka University Graduate School of Medicine, 2-2 Yamada-oka, Suita, Osaka 565-0871, Japan. E-mail: takehara@gh.med.osaka-u.ac.jp; Fax: (81)-6-6879-3629.

DOI 10.1002/hep.24305

Potential conflict of interest: Nothing to report.

Additional Supporting Information may be found in the online version of this article.

obtained from Cell Signaling Technology (Beverly, MA); anti-Bax and anti-cIAP2 antibodies were obtained from Millipore (Billerica, MA); anti-Bid antibody, which detects truncated Bid, was generously provided by Xiao-Ming Yin (Indiana University School of Medicine, Indianapolis, IN)[17]; and anti–β-actin antibody was obtained from Sigma-Aldrich. For isolation of the mitochondria-rich fraction, a Mitochondrial Isolation Kit (Thermo Scientific, Rockford, IL) was used. The isolation of hepatocytes from whole liver has been described.[13]

Detection of Bax Oligomerization. Liver tissue was lysed with HCN buffer (25 mM 4-(2-hydroxyethyl)-1-piperazine ethanesulfonic acid, 300 mM NaCl, 2% CHAPS, protease inhibitor cocktail, phosphatase inhibitor cocktail, 100 μM BOC-Asp(OMe)CH2F [MP Biomedicals, Solon, OH]; pH 7.5). After the liver lysate was sonicated and centrifuged, the supernatant was collected and the concentration was adjusted. For cross-linking, 100 μL of the lysate was incubated with 5 μL 100 mM bis(maleimido)hexane (Thermo Scientific) and 5 μL 100 mM BS^3 (Thermo Scientific) for 30 minutes at room temperature as described.[18] After quenching the cross-linkers by way of incubation with 12 μL 1 M Tris-HCl (pH 7.5) for 15 minutes at room temperature, the lysate was boiled with sample buffer followed by western blot analysis for Bax.

Electron Microscopy. Livers were fixed by perfusion of phosphate-buffered saline with 2.5% glutaraldehyde solution buffered at pH 7.4 with 0.1 M Millonig's phosphate, postfixed in 1% osmium tetroxide solution at 4°C for 1 hour, dehydrated in graded concentrations of ethanol, and embedded in Quetol 812 epoxy resin (Nisshin EM, Tokyo, Japan). Ultrathin sections (80 nm) cut on ultramicrotome were stained with uranyl acetate and lead citrate and examined with an H-7650 electron microscope (Hitachi Ltd., Tokyo, Japan) at 80 kV.

Statistical Analysis. Data are presented as the mean ± SE. Differences between two groups were determined using the Mann-Whitney U test for unpaired observations. The survival curves were estimated using the Kaplan-Meier method and were tested by way of log-rank test. $P < 0.05$ was considered statistically significant.

Results

Bak Deficiency Partially Ameliorates Fas-Induced Hepatocellular Apoptosis but Fails to Prevent Animal Death. First, to examine the significance of Bak in hepatocellular apoptosis induced by Fas stimulation, Bak KO mice ($bak^{-/-}$) and wild-type (WT) littermates ($bak^{+/+}$) were intraperitoneally injected with 1.5 mg/kg Jo2 anti-Fas antibody and analyzed 3 hours later. Consistent with previous reports,[10,19] WT mice showed severe elevation of serum ALT levels with massive hepatocellular apoptosis (Fig. 1A,B). Bak KO mice also developed liver injury, but the levels of serum ALT and the number of TUNEL-positive hepatocytes were significantly lower in Bak KO mice than in WT mice (Fig. 1A-C). Western blotting for cleaved caspase-3, caspase-7, and PARP revealed that activation of effector caspases were partially inhibited in KO livers compared with WT livers (Fig. 1D). Cleavage of procaspase-9, which is initiated by mitochondrial release of cytochrome c, was also suppressed in Bak KO livers compared with WT liver (Fig. 1D). The cleaved form of caspase-8, a direct downstream target of Fas activation, was detected in both mice, but its levels were reduced in Bak KO mice compared with WT mice (Fig. 1D). This reduction may be explained by the lesser activation of caspase-3/7, because it has been reported that caspase-3/7 could activate caspase-8 through an amplification loop during apoptosis.[20] Collectively, these findings demonstrated that Bak deficiency partially ameliorated Fas-induced hepatocellular apoptosis associated with reduced cleavage of caspase-9, caspase-3/7, and PARP. We then compared survival of mice after Jo2 injection but found that Bak KO mice also rapidly died with kinetics similar to those of WT mice, suggesting that partial amelioration of hepatocellular apoptosis induced by Bak deficiency did not lead to survival benefit under our experimental conditions (Fig. 1E). Because Bax residing in the cytosol moves to the mitochondria upon activation, where it undergoes oligomerization,[21] we analyzed its translocation and oligomerization in the liver at 3 hours after Jo2 injection. Western blot analysis revealed that the levels of Bax expression clearly increased in the mitochondrial fraction in both WT livers and Bak KO livers (Fig. 1F). Signals for the Bax dimer were also detected in both livers (Fig. 1F). These findings indicate that Bax is also activated after Fas stimulation, raising the possibility of its involvement in hepatocellular apoptosis.

Bax Deficiency Fails to Ameliorate Fas-Induced Hepatocellular Apoptosis. Next, to examine the significance of Bax in hepatocellular apoptosis induced by Fas stimulation, Bax KO mice ($bax^{-/-}$) and WT littermates ($bax^{+/+}$) were injected with Jo2 and examined 3 hours later. There was no significant difference in the levels of serum ALT or the number of TUNEL-positive hepatocytes between the two groups (Fig. 2A-C), which is consistent with a previous report.[22] The levels of the cleaved forms of caspase-8, -9, -3, -7, and

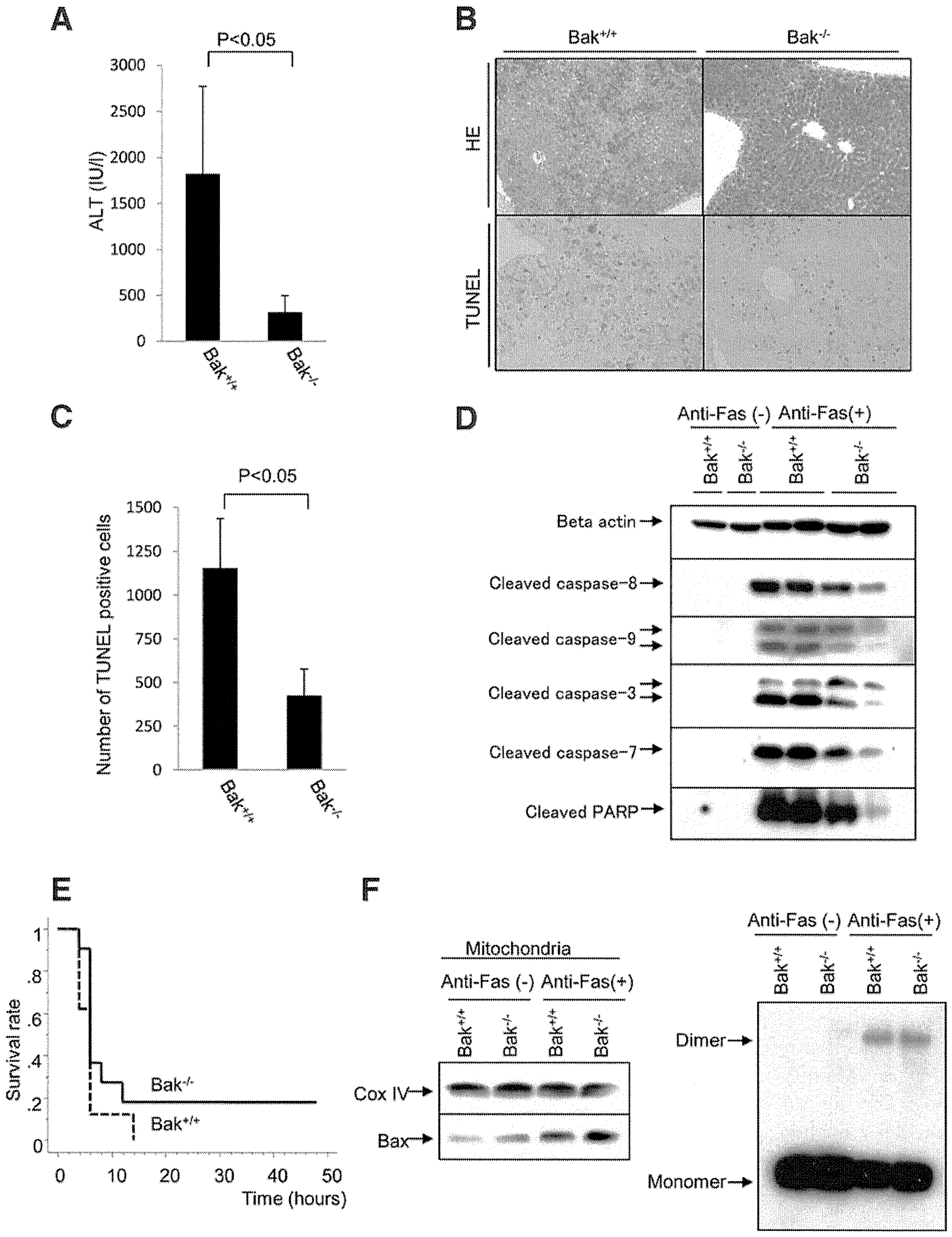

Fig. 1. Bak KO mice are partially resistant to Fas-induced hepatocellular apoptosis. Bak KO mice (Bak$^{-/-}$) or control WT littermates (Bak$^{+/+}$) were analyzed at 3 hours after intraperitoneal injection of 1.5 mg/kg Jo2 anti-Fas antibody. (A) Serum ALT levels (n = 10 or 11, respectively). (B) Hematoxylin and eosin (HE) and TUNEL staining of the liver sections. (C) Number of TUNEL-positive cells (n = 8 or 9, respectively). (D) Western blot analysis for the expressions of cleaved caspase-8, 9, -3, -7 and PARP. (E) Bak KO mice or control WT littermates were intraperitoneally injected with 1.5 mg/kg Jo2 anti-Fas antibody (n = 8 or 11, respectively). Survival rates after Jo2 injection are shown. (F) Bak KO mice or control WT littermates were analyzed 3 hours after intraperitoneal injection of Jo2 anti-Fas antibody (1.5 mg/kg) or vehicle. Left: Western blot analysis of the mitochondrial fraction of the liver for the expression of Bax. Right: Western blot analysis for the expression of Bax monomer and dimer in the liver.

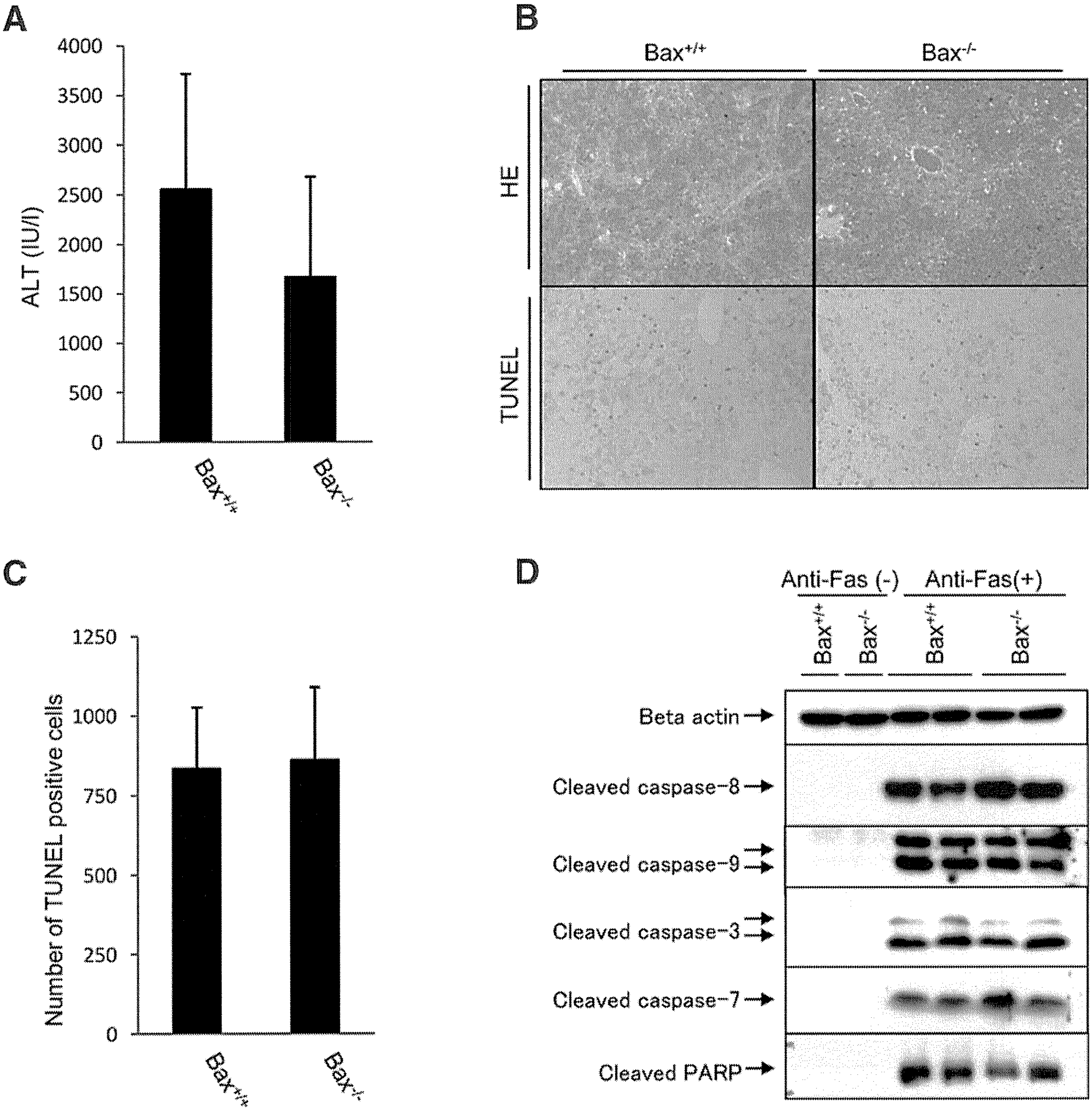

Fig. 2. Bax KO mice are not resistant to Fas-induced hepatocellular apoptosis. Bax KO mice ($Bax^{-/-}$) or control WT littermates ($Bax^{+/+}$) were analyzed 3 hours after intraperitoneal injection of Jo2 anti-Fas antibody (1.5 mg/kg). (A) Serum ALT levels ($n = 11$ per group). (B) Hematoxylin and eosin (HE) and TUNEL staining of the liver sections. (C) Number of TUNEL-positive cells ($n = 8$ per group). (D) Western blot analysis for the expressions of cleaved caspase-8, -9, -3, -7, and PARP.

PARP in Bax KO livers did not differ from those of WT livers (Fig. 2D). These findings demonstrate that, in contrast to Bak deficiency, Bax deficiency was not able to inhibit Fas-induced hepatocellular apoptosis.

Bax Deficiency Completely Blocks Fas-Induced Early-Onset Hepatocellular Apoptosis in a Bak-Deficient Background. To examine the impact of Bax in a Bak-deficient background, hepatocyte-specific Bak/Bax DKO mice ($bak^{-/-}$ $bax^{flox/flox}$ *Alb-Cre*) and Bak KO mice ($bak^{-/-}$ $bax^{flox/flox}$), which served as control littermates of this mating, were injected with Jo2 and analyzed 3 hours later. We confirmed the hepatocyte-specific defects of Bax protein in Bak/Bax DKO mice by way of western blot analysis (Fig. 3A). The serum ALT levels of Bak/Bax DKO mice were in the normal range and were significantly lower than those of Bak KO mice (Fig. 3B). Liver histology and TUNEL staining did not show evidence of hepatocyte apoptosis in Bak/Bax DKO livers, in contrast to Bak KO livers (Fig. 3C,D). Taken together, these results indicate that Bak and Bax are basically redundant molecules for execution of hepatocellular apoptosis induced by Fas

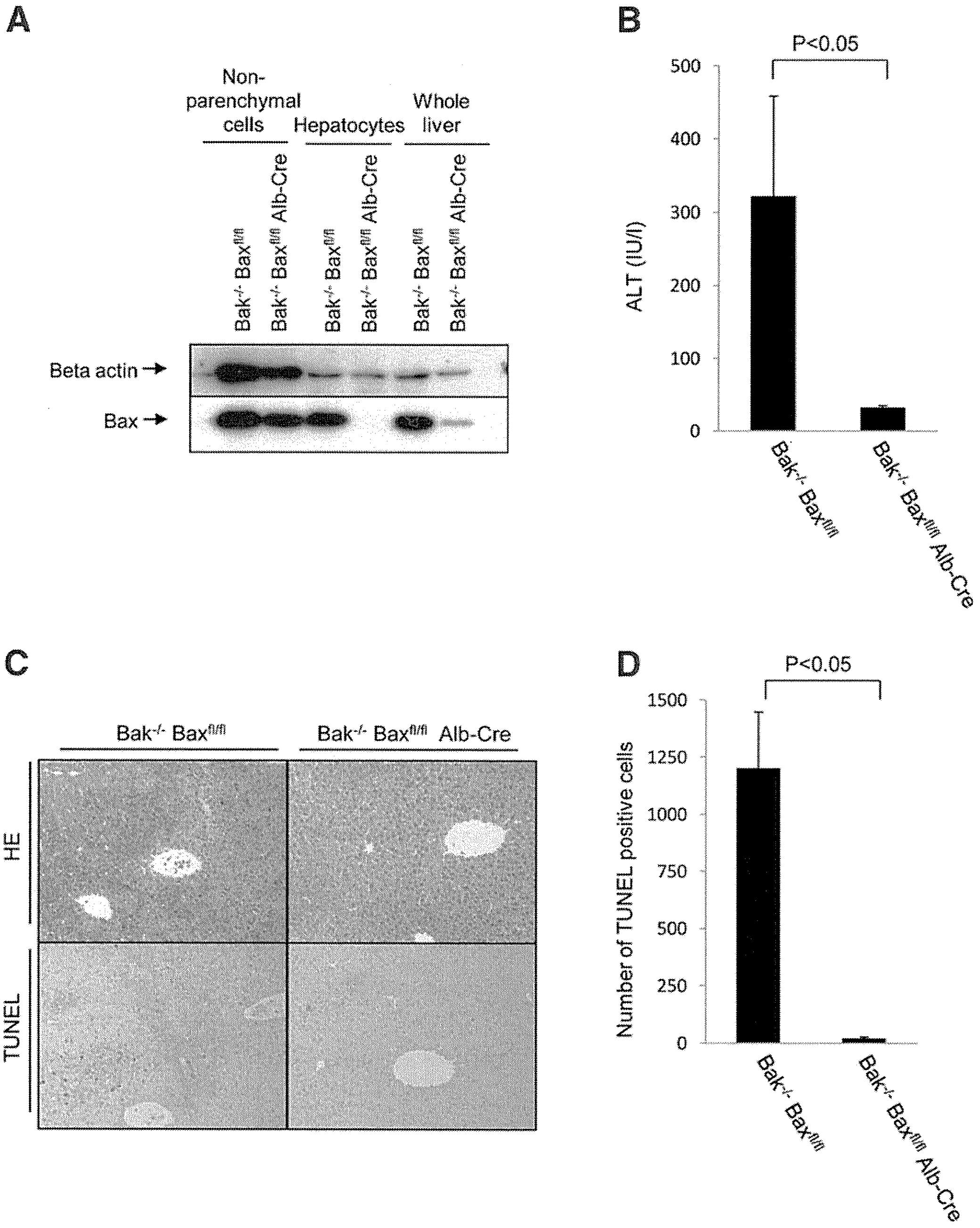

Fig. 3. Bak/Bax DKO mice are fully resistant to Fas-induced hepatocellular apoptosis in early phase. (A) Western blot analysis of the indicated fraction of the liver for the expressions of Bax. (B-D) Bak/Bax DKO mice (Bak$^{-/-}$ Bax$^{fl/fl}$ Alb-Cre) or control Bak KO littermates (Bak$^{-/-}$ Bax$^{fl/fl}$) were analyzed 3 hours after intraperitoneal injection of Jo2 anti-Fas antibody (1.5 mg/kg). (B) Serum ALT levels (n = 10 per group). (C) Hematoxylin and eosin (HE) and TUNEL staining of the liver sections. (D) Number of TUNEL-positive cells (n = 9 per group).

activation, although the former appears to be clearly required for full-blown apoptosis in vivo.

Fas Stimulation Leads to Late-Onset Hepatocellular Death Even in Bak/Bax Deficiency with Moderate Caspase-3/7 Activation Without Mitochondrial Disruption. To examine whether the inhibition of Fas-induced rapid liver injury in Bak/Bax deficiency is a durable effect, we analyzed the survival rate after Jo2 injection. The survival rate of Bak/Bax DKO mice was significantly higher than that of Bak KO mice, but approximately half of the Bak/Bax DKO mice died within 12 hours (Fig. 4A). To examine the cause of this late-onset lethality, we analyzed the serum ALT levels and liver tissue 6 hours after Jo2 injection. Unexpectedly, the serum ALT levels were highly elevated in Bak/Bax DKO mice (Fig. 4B). Liver histology revealed many hepatocytes with cellular shrinkage and scattered regions of sinusoidal hemorrhage (Fig. 4C), indicating that Bak/Bax DKO mice still developed severe liver injury at this time point. TUNEL staining

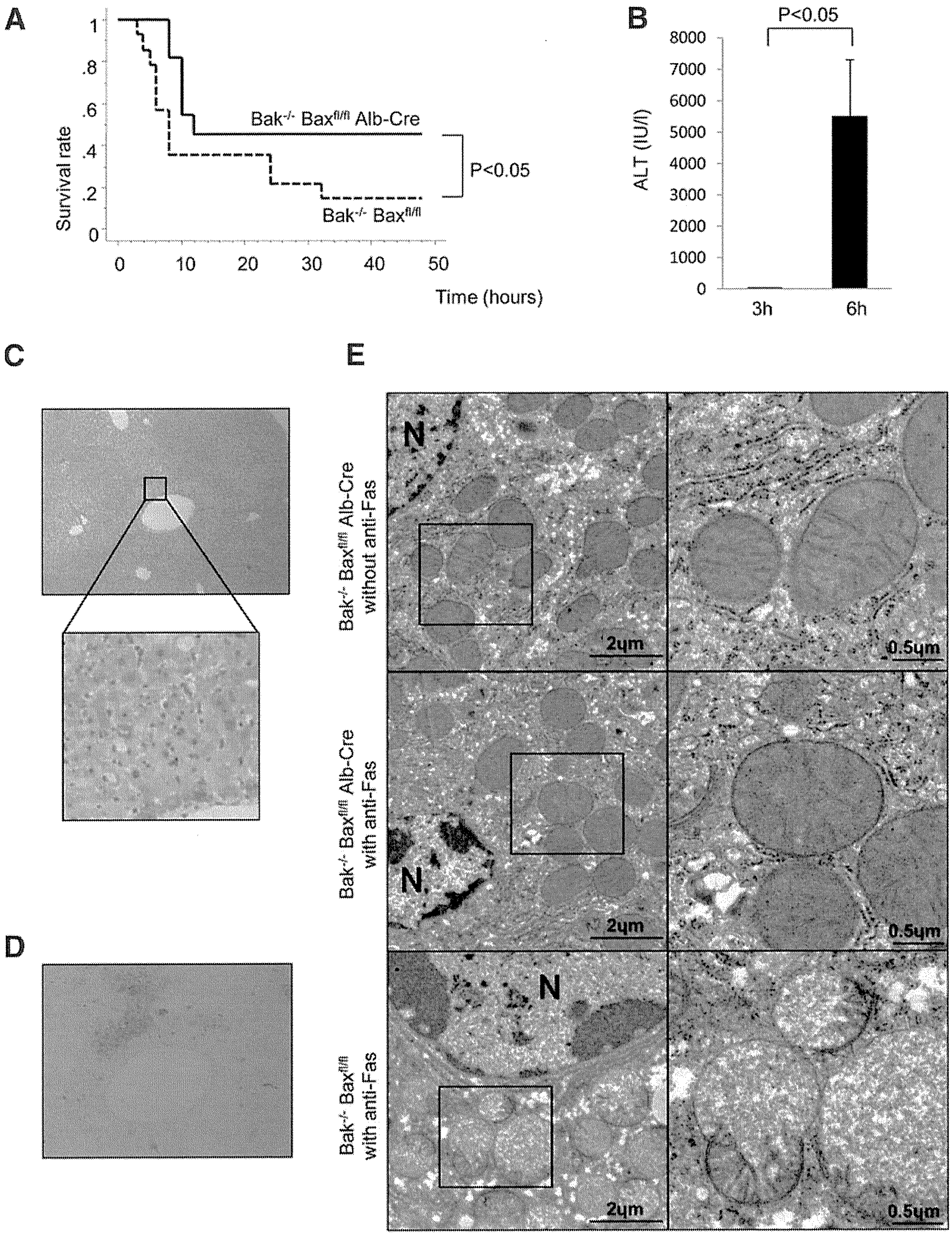

Fig. 4. Bak/Bax DKO mice develop late-onset severe liver injury upon Fas stimulation. Bak/Bax DKO mice (Bak$^{-/-}$ Bax$^{fl/fl}$ Alb-Cre) or control Bak KO littermates (Bak$^{-/-}$ Bax$^{fl/fl}$) were intraperitoneally injected with 1.5 mg/kg Jo2 anti-Fas antibody. (A) Survival rate after Jo2 injection (n = 11 per group). (B) Serum ALT levels of Bak/Bax DKO mice. (C, D) Hematoxylin and eosin (C) and TUNEL (D) staining of the liver sections of Bak/Bax DKO mice 6 hours after Jo2 injection. Representative photomicrographs are shown. (E) Representative electron microscopy photomicrographs of the livers of Bak/Bax DKO mice before and 6 hours after Jo2 anti-Fas injection (1.5 mg/kg) and control Bak KO mice 2 hours after Jo2 anti-Fas injection (1.5 mg/kg). Right panels are enlarged images of the square area of each left panel. N, nucleus.

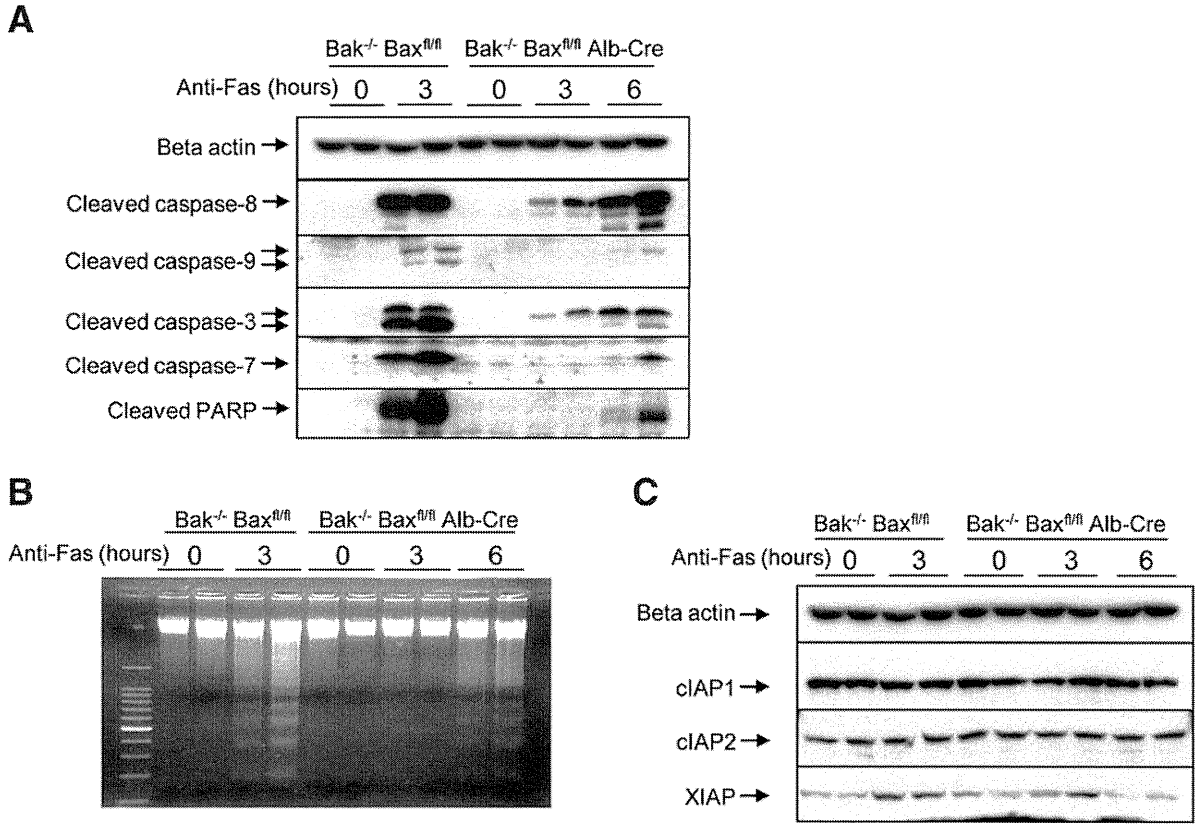

Fig. 5. Fas-mediated hepatocellular death in Bak/Bax DKO mice is associated with caspase-3/7 activation and oligonucleosomal DNA breaks. Bak/Bax DKO mice (Bak$^{-/-}$ Bax$^{fl/fl}$ Alb-Cre) or control Bak KO littermates (Bak$^{-/-}$ Bax$^{fl/fl}$) were intraperitoneally injected with Jo2 anti-Fas antibody (1.5 mg/kg). (A) Western blot analysis for expression of cleaved caspase-8, -9, -3, -7, and PARP. (B) DNA laddering of the liver. (C) Western blot analysis for expression of IAP family proteins.

revealed many TUNEL-positive hepatocytes in the liver sections. Of importance, electron microscopic analysis revealed mitochondrial alterations (such as disruption of the membrane and herniation of the matrix) in hepatocytes of Bak KO mice but not in hepatocytes of Bak/Bax DKO mice with chromatin condensation (Fig. 4E). Because some reports showed that hepatocytes act like type I cells with a high dose of Jo2 anti-Fas antibody and that anti-Fas antibody does not always reliably mimic the action of the physiological Fas ligand,[23,24] we also injected 0.5 mg/kg Jo2 or recombinant Fas ligand into Bak/Bax DKO mice. Similarly, both injected mice showed severe elevation of serum ALT levels and severe hepatitis with many TUNEL-positive cells at 6 hours (Supporting Figs. 1 and 2).

To examine the kinetics of caspase activation and apoptosis in the liver after Jo2 administration, we performed western blot analysis for caspase activation and agarose gel electrophoresis for DNA laddering. All signals for cleaved forms of caspase-3, caspase-7, and PARP in the liver were clearly detected at 6 hours in Bak/Bax DKO mice, although they were weaker than those at 3 hours in control Bak KO littermates (Fig. 5A). Regarding the cleaved form of caspase-9, two bands were detected at 3 hours in Bak KO liver, but not in Bak/Bax DKO liver. Previous research established that procaspase-9 has two sites for cleavage upon activation: both Asp353 and Asp368 sites are autoprocessed by caspase-9 activation after cytochrome c release, whereas the Asp368 site is preferentially processed over the Asp358 site by caspase-3.[25] In our western blot analysis, the slow migrating species corresponding to the fragment cleaved at Asp368, but not the rapid migrating species corresponding to that at Asp353, was weakly detected at 6 hours in Bak/Bax DKO liver. This indicated that caspase-3–mediated cleavage of procaspase-9 takes place without evidence of cytochrome c–induced autoprocessing of procaspase-9. Agarose gel electrophoresis clearly detected oligonucleosomal DNA laddering at 6 hours in Bak/Bax DKO livers, similar to our observation at 3 hours in control Bak KO livers (Fig. 5B). Collectively, these morphological and biochemical data support the idea that hepatocellular death occurring at 6 hours in the Bak/Bax DKO liver seems to involve apoptosis.

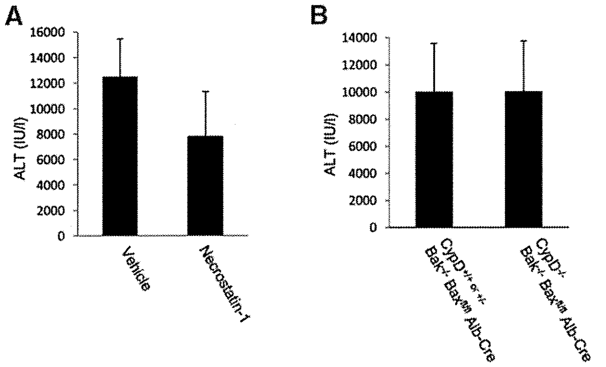

Fig. 6. Fas-induced hepatocellular death in Bak/Bax DKO mice is independent of RIP kinase and/or CypD. (A) Bak/Bax DKO mice ($Bak^{-/-}$ $Bax^{fl/fl}$ Cre) were intraperitoneally injected with 2 mg/kg necrostatin-1 in vehicle containing 0.2% dimethylsulfoxide or vehicle alone at 2 hours after injection of 1.5 mg/kg Jo2 anti-Fas antibody. Serum ALT levels at 6 hours after Jo2 injection are shown (n = 8 per group). (B) $CypD^{+/+ \text{ or } +/-}$ mice in a Bak/Bax-deficient background ($CypD^{+/+ \text{ or } +/-}$ $Bak^{-/-}$ $Bax^{fl/fl}$ Alb-Cre) or control $CypD^{-/-}$ littermates ($CypD^{-/-}$ $Bak^{-/-}$ $Bax^{fl/fl}$ Alb-Cre) were intraperitoneally injected with 1.5 mg/kg Jo2 anti-Fas antibody. Serum ALT levels at 6 hours after injection are shown (n = 7 per group or 8 per group, respectively).

To examine the underlying mechanisms by which caspase-3/7 was increasingly activated from 3 to 6 hours in Bak/Bax DKO mice, we analyzed the expression of inhibition of apoptosis proteins (IAPs), which can block cleavage of procaspase-3, -7, and -9.[26] The expression levels of cIAP1 and cIAP2 were not changed in the liver after Jo2 injection (Fig. 5C, Supporting Fig. 3). In contrast, the expression levels of XIAP were up-regulated in the livers of both Bak KO and Bak/Bax DKO mice at 3 hours after Jo2 injection, as in WT mice (Fig. 5C, Supporting Fig. 3), which is consistent with previous reports.[27] However, this up-regulation disappeared from the livers of Bak/Bax DKO mice at 6 hours. Repression of XIAP overexpression might explain why weak activation of capsase-3/7 gradually increased from 3 to 6 hours in the Bak/Bax DKO liver.

Cell Death with Bak/Bax Deficiency Is Not Dependent on a Necrotic Pathway. Fas activation was reported to induce not only caspase-dependent apoptosis but also caspase-independent necrosis, which is required for receptor-interacting protein (RIP) kinase.[28] To exclude the possibility of this necrotic cell death in the Bak/Bax DKO liver, we first examined the effect of necrostatin-1, which specifically inhibits RIP kinase to protect against necrotic cell death caused by death-domain receptor stimulation.[2,29] Bak/Bax DKO mice were injected with 2 mg/kg necrostatin-1 at 2 hours after or 1 hour before Jo2 injection. The ALT levels at 6 hours after Fas stimulation were clearly elevated without a significant difference between the necrostatin-1 injection group and the vehicle injection group (Fig. 6A and Supporting Fig. 4). We next examined the effect of CypD, which is a key molecule of mitochondrial permeability transition generated by Ca^{2+} overload and/or oxidative stress leading to necrotic cell death.[14,30] We injected Jo2 into $CypD^{-/-}$ mice with a Bak/Bax-deficient background (*$cypd^{-/-}$ $bak^{-/-}$ $bax^{flox/flox}$ Alb-Cre*) or control $CypD^{+/+ \text{ or } +/-}$ littermates (*$cypd^{+/+ \text{ or } +/-}$ $bak^{-/-}$ $bax^{flox/flox}$ Alb-Cre*). The ALT levels of CypD/Bak/Bax triple KO mice upon Fas stimulation were the same as those of control mice (Fig. 6B). These results indicate that liver injury in Bak/Bax deficiency induced by Fas stimulation was not dependent on the necrotic pathway, at least that mediated by RIP kinase and/or CypD.

Late-Onset Cell Death in Bak/Bax Deficiency Is Completely Dependent on Caspase. Although cell death observed in Bak/Bax DKO mice appears to be apoptosis, the question arose of whether relatively weak caspase-3/7 activity compared with that observed in Bak KO mice is sufficient for inducing liver injury 6 hours after Fas simulation. To this end, Bak/Bax DKO mice were given 40 mg/kg Q-VD-Oph, a potent broad spectrum caspase inhibitor,[31] 2 hours after injection of Jo2. Western blot analysis revealed the existence of truncated Bid and cleaved caspase-8 in the liver 2 hours after Jo2 injection, demonstrating that caspase-8 had already been activated by this point (Fig. 7A). Administration of the caspase inhibitor at 2 hours completely blocked the elevation of serum ALT levels and hepatocellular apoptosis, as evidenced by liver histology and TUNEL staining 6 hours after Jo2 injection (Fig. 7B-D). Finally, we tried to analyze the survival rate of Bak/Bax DKO mice and control Bak KO mice when therapeutically injected with the caspase inhibitor 2 hours after Jo2 injection. None of the Bak/Bax DKO mice showed lethal liver injury upon Jo2 injection, whereas half of the Bak KO mice died from severe liver injury (Fig. 7E). These findings suggest that Fas-induced liver injury in Bak/Bax deficiency was dependent on caspase activity, which could be fully negated by the caspase inhibitor. On the other hand, caspase activation in Bak KO mice was too high to be negated by the same dose of the caspase inhibitor.

Discussion

In the present study, we demonstrate that Bak KO, but not Bax KO, provides partial resistance to Fas-induced hepatocellular apoptosis in vivo. We demonstrated previously that Bak KO mice, but not Bax KO

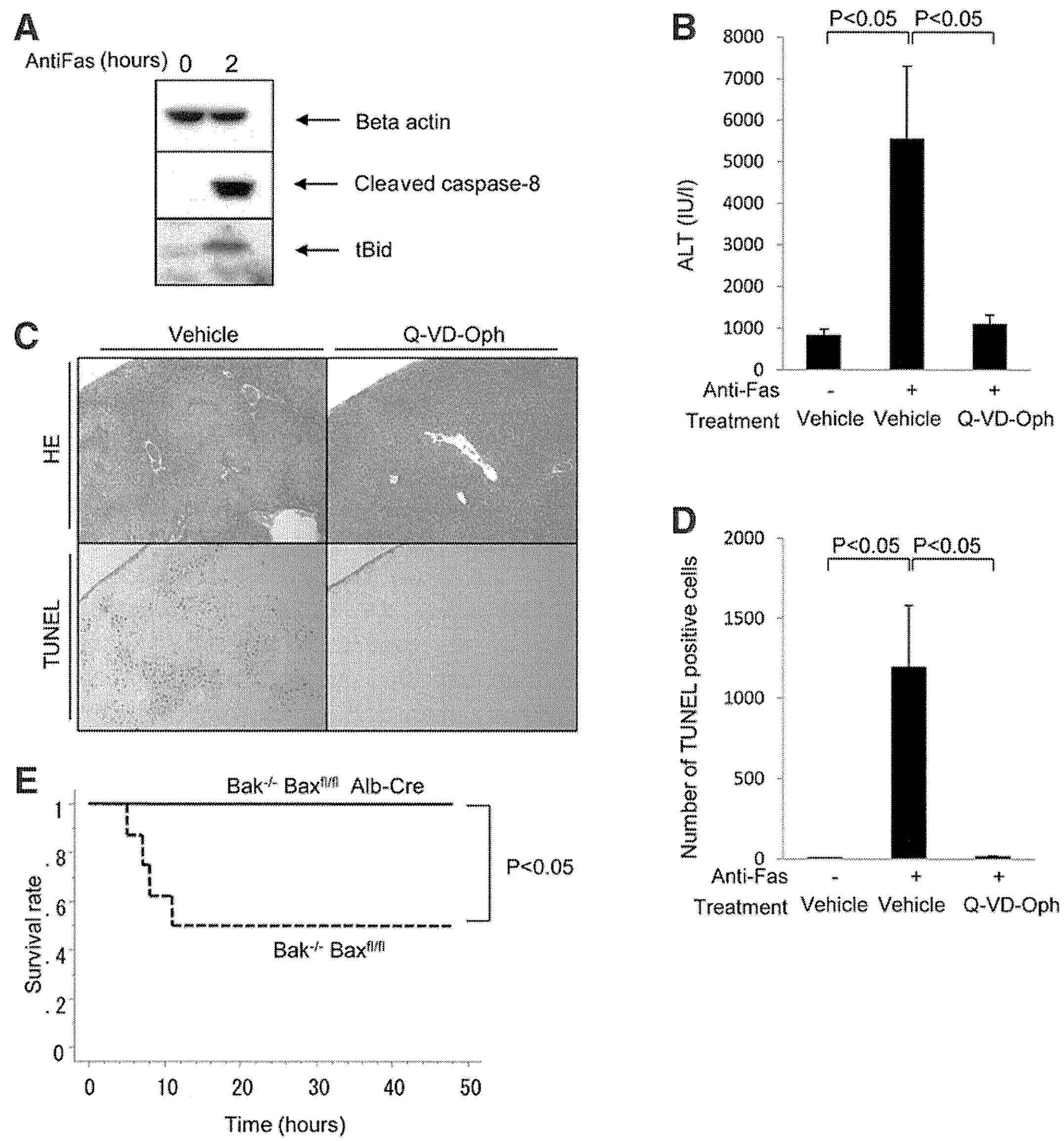

Fig. 7. Hepatocellular death in Bak/Bax DKO mice is dependent on caspase activation. (A) Bak/Bax DKO mice were analyzed before and 2 hours after intraperitoneal injection of Jo2 anti-Fas antibody (1.5 mg/kg). Western blot analysis of the liver for the expression of cleaved caspase-8 and truncated Bid (tBid). (B-D) Bak/Bax DKO mice were intraperitoneally administered 40 mg/kg Q-VD-Oph in 10 mL/kg dimethylsulfoxide (DMSO) or DMSO alone, as a vehicle, 2 hours after injection of 1.5 mg/kg Jo2 anti-Fas antibody and analyzed at 6 hours. (B) Serum ALT levels (n = 6 or 7 per group, respectively). (C) Hematoxylin and eosin (HE) and TUNEL staining of the liver sections. (D) Number of TUNEL-positive cells (n = 6 or 7 per group, respectively). Because intraperitoneal injection of DMSO leads to injury at the surface layer of the liver, TUNEL positivity close to the surface layer was excluded from the cell count. (E) Bak/Bax DKO mice (Bak$^{-/-}$ Bax$^{fl/fl}$ Alb-Cre) or control Bak KO littermates (Bak$^{-/-}$ Bax$^{fl/fl}$) were given 40 mg/kg Q-VD-Oph intraperitoneally in 10 mL/kg DMSO or DMSO alone at 2 hours after injection of 1.5 mg/kg anti-Fas antibody. The disease-free survival rate of lethal liver injury after Jo2 injection is shown (n = 8 per group).

mice, showed resistance to apoptosis induced by Bcl-xL deficiency, which depended mainly on Bid activation.[16] Research has shown that Fas induces apoptosis in hepatocytes through the Bid pathway,[10,11] and the present study also demonstrates that Bid becomes truncated in the liver upon anti-Fas injection. Therefore, truncated Bid may preferentially activate Bak rather than Bax in the liver. However, the present study also reveals that, in the absence of Bak, Bax plays an essential role in mediating the early onset of hepatocellular apoptosis. The most important finding of this study is that Bak/Bax deficiency failed to protect against the late onset of liver injury after Jo2 anti-Fas injection as well as Fas agonist injection. Wei et al.,[32] in their historical paper establishing the importance of Bak and Bax in the mitochondrial pathway of apoptosis, reported that hepatocytes were protected from Jo2-induced apoptosis in traditional Bak/Bax DKO mice (*bak*$^{-/-}$ *bax*$^{-/-}$). Because perinatal lethality occurs with most traditional Bak/Bax DKO mice, they could only analyze three animals, which did not enable detailed analysis of cell death due to Jo2 stimulation. The present study is the first to (1) thoroughly examine the impact of Bak and Bax in the liver using conditional KO mice and (2) demonstrate that Bak/Bax deficiency can protect against Fas-induced severe injury in the early phase but not in the late phase.

The late onset of liver injury observed in Bak/Bax DKO appeared to be apoptosis based on biochemical and morphological observations, including caspase activation, oligonucleosomal DNA breaks and, most importantly, identification of cell death with caspase dependency. In addition, the well-established necrotic pathway mediated by RIP kinase and/or CypD was not involved. However, the difference from apoptosis observed in Bak KO mice was the absence of mitochondrial alteration or cytochrome c–dependent caspase-9 processing in Bak/Bax DKO mice. We also confirmed that Bak/Bax-deficient mitochondria were not capable of releasing cytochrome c in the presence of truncated Bid (Supporting Fig. 5). These data support the idea that activation of the mitochondrial pathway of apoptosis is fully dependent on either Bak or Bax even in the late phase, indicating at the same time that late onset of apoptosis takes place through an extrinsic pathway rather than the mitochondrial pathway.

Although hepatocytes are generally considered to be type II cells, recent work has shown that the requirement of the mitochondrial pathway may be overcome through changes induced by in vitro culture conditions[33,34] or the strength of Fas stimulation.[23] Schüngel et al.[23] demonstrated that hepatocytes act as type II cells with a low-dose Jo2 injection (0.5 mg/kg) and act as type I cells with an extremely high-dose Jo2 injection (5 mg/kg). This agrees with the generally accepted idea that type I cells exhibit strong activation of DISC and caspase-8, which itself is sufficient to induce apoptosis, whereas type II cells exhibit weak activation and therefore require amplification of the apoptosis signal through the mitochondrial loop. In the present study, we used 1.5 mg/kg or 0.5 mg/kg Jo2 antibody, which could be considered relatively low doses, and found that hepatocytes act like type II cells in WT mice or Bak/Bax single KO mice but act like type I cells in Bak/Bax DKO mice. The present study therefore demonstrates that hepatocytes can act as type I cells in the absence of Bak and Bax independent of the strength of DISC formation or signals from microenvironments.

The question arises of why hepatocytes can act as type I cells where the levels of DISC formation or caspase-8 activation may be insufficient to induce activation of downstream caspases. Recently, Jost et al.[27] reported a discriminating role of XIAP between type I and type II cells; in type II cells, the levels of XIAP expression increased after Fas stimulation but decreased in type I cells. In agreement with this report, XIAP expression was up-regulated at 3 hours in both Bak KO and Bak/Bax DKO livers. Interestingly, this XIAP up-regulation disappeared at 6 hours after Jo2 injection in Bak/Bax DKO mice. Because XIAP is a potent inactivator of caspase-3, -7, and -9 processing, repression of XIAP may be one reason why hepatocytes can act as type I cells at this time point.

Previous studies have reported that liver endothelial cells express Fas receptor and have suggested that apoptosis of these cells may participate in the liver damage in mice receiving Jo2 antibody, especially in the case of high-dose administration.[35] However, we did not find liver injury in the sinusoidal hemorrhage in Bak/Bax DKO mice at 3 hours after Jo2 injection, which is the time point when Bak KO mice developed it (Fig. 3C). Together with the fact that Bax, but not Bak, was active in liver nonparenchymal cells in our Bak/Bax DKO mice, as was the case in Bak KO mice (Fig. 3A), we speculate that Bak-deficient sinusoidal cells could not contribute much to liver injury at 3 hours after Jo2 injection (1.5 or 0.5 mg/kg).

Recently, a pan-caspase inhibitor was reported to reduce hepatic damage in liver transplant recipients and patients with chronic hepatitis C in clinical trials.[36,37] For treatment of fulminant liver injury, caspase inhibitors seem to be attractive drugs. However, the present study demonstrates that Fas-induced apoptotic signals could be efficiently amplified through the mitochondrial pathway, leading to high lethality even if caspase inhibitor was administered 2 hours after Jo2 injection. In contrast, administration of the same dose of the caspase inhibitor was able to fully block hepatocyte apoptosis and lethality in Bak/Bax DKO mice. From a clinical point of view, when using caspase inhibitors to prevent fulminant liver failure, concomitant inactivation of the mitochondrial amplification loop may be required.

In conclusion, the extrinsic pathway of apoptosis exists in hepatocytes and causes late onset of lethal liver failure in the absence of Bak and Bax independent of the strength of Fas ligation. This pathway could be therapeutically intervened through the use of caspase inhibitors, presumably due to low levels of DISC formation and subsequent weak activation of effector caspases in hepatocytes. The present study unveils the entire framework of the Fas-mediated signaling pathway in hepatocytes, placing the mitochondrial pathway of apoptosis as a potent loop for amplifying activation of the caspase cascade to execute complete and rapid cell death in hepatocytes.

Acknowledgment: We thank Xiao-Ming Yin (Department of Pathology and Laboratory Medicine, Indiana University School of Medicine) for providing the anti-mouse Bid antibody.

References

1. Guicciardi M, Gores G. Life and death by death receptors. FASEB J 2009;23:1625-1637.
2. Malhi H, Guicciardi M, Gores G. Hepatocyte death: a clear and present danger. Physiol Rev 2010;90:1165-1194.
3. Hiramatsu N, Hayashi N, Katayama K, Mochizuki K, Kawanishi Y, Kasahara A, et al. Immunohistochemical detection of Fas antigen in liver tissue of patients with chronic hepatitis C. HEPATOLOGY 1994;19: 1354-1359.
4. Hayashi N, Mita E. Involvement of Fas system-mediated apoptosis in pathogenesis of viral hepatitis. J Viral Hepat 1999;6:357-365.
5. Feldstein A, Canbay A, Angulo P, Taniai M, Burgart L, Lindor K, et al. Hepatocyte apoptosis and fas expression are prominent features of human nonalcoholic steatohepatitis. Gastroenterology 2003;125: 437-443.
6. Ryo K, Kamogawa Y, Ikeda I, Yamauchi K, Yonehara S, Nagata S, et al. Significance of Fas antigen-mediated apoptosis in human fulminant hepatic failure. Am J Gastroenterol 2000;95:2047-2055.
7. Feldmann G, Lamboley C, Moreau A, Bringuier A. Fas-mediated apoptosis of hepatic cells. Biomed Pharmacother 1998;52:378-385.
8. Tsujimoto Y. Cell death regulation by the Bcl-2 protein family in the mitochondria. J Cell Physiol 2003;195:158-167.
9. Tait S, Green D. Mitochondria and cell death: outer membrane permeabilization and beyond. Nat Rev Mol Cell Biol 2010;11:621-632.
10. Yin X, Wang K, Gross A, Zhao Y, Zinkel S, Klocke B, et al. Bid-deficient mice are resistant to Fas-induced hepatocellular apoptosis. Nature 1999;400:886-891.
11. Kaufmann T, Tai L, Ekert PG, Huang DC, Norris F, Lindemann RK, et al. The BH3-only protein bid is dispensable for DNA damage- and replicative stress-induced apoptosis or cell-cycle arrest. Cell 2007;129: 423-433.
12. Lindsten T, Ross A, King A, Zong W, Rathmell J, Shiels H, et al. The combined functions of proapoptotic Bcl-2 family members bak and bax are essential for normal development of multiple tissues. Mol Cell 2000;6:1389-1399.
13. Takehara T, Tatsumi T, Suzuki T, Rucker EB, 3rd, Hennighausen L, Jinushi M, et al. Hepatocyte-specific disruption of Bcl-xL leads to continuous hepatocyte apoptosis and liver fibrotic responses. Gastroenterology 2004;127:1189-1197.
14. Nakagawa T, Shimizu S, Watanabe T, Yamaguchi O, Otsu K, Yamagata H, et al. Cyclophilin D-dependent mitochondrial permeability transition regulates some necrotic but not apoptotic cell death. Nature 2005; 434:652-658.
15. Hikita H, Takehara T, Shimizu S, Kodama T, Li W, Miyagi T, et al. Mcl-1 and Bcl-xL cooperatively maintain integrity of hepatocytes in developing and adult murine liver. HEPATOLOGY 2009;50:1217-1226.
16. Hikita H, Takehara T, Kodama T, Shimizu S, Hosui A, Miyagi T, et al. BH3-only protein bid participates in the Bcl-2 network in healthy liver cells. HEPATOLOGY 2009;50:1972-1980.
17. Wang K, Yin X, Chao D, Milliman C, Korsmeyer S. BID: a novel BH3 domain-only death agonist. Genes Dev 1996;10:2859-2869.
18. Yamagata H, Shimizu S, Nishida Y, Watanabe Y, Craigen WJ, Tsujimoto Y. Requirement of voltage-dependent anion channel 2 for pro-apoptotic activity of Bax. Oncogene 2009;28:3563-3572.
19. Ogasawara J, Watanabe-Fukunaga R, Adachi M, Matsuzawa A, Kasugai T, Kitamura Y, et al. Lethal effect of the anti-Fas antibody in mice. Nature 1993;364:806-809.
20. Wieder T, Essmann F, Prokop A, Schmelz K, Schulze-Osthoff K, Beyaert R, et al. Activation of caspase-8 in drug-induced apoptosis of B-lymphoid cells is independent of CD95/Fas receptor-ligand interaction and occurs downstream of caspase-3. Blood 2001;97:1378-1387.
21. Antonsson B, Montessuit S, Sanchez B, Martinou J. Bax is present as a high molecular weight oligomer/complex in the mitochondrial membrane of apoptotic cells. J Biol Chem 2001;276:11615-11623.
22. Kim T, Zhao Y, Barber M, Kuharsky D, Yin X. Bid-induced cytochrome c release is mediated by a pathway independent of mitochondrial permeability transition pore and Bax. J Biol Chem 2000;275: 39474-39481.
23. Schüngel S, Buitrago-Molina L, Nalapareddy P, Lebofsky M, Manns M, Jaeschke H, et al. The strength of the Fas ligand signal determines whether hepatocytes act as type 1 or type 2 cells in murine livers. HEPATOLOGY 2009;50:1558-1566.
24. Huang DC, Hahne M, Schroeter M, Frei K, Fontana A, Villunger A, et al. Activation of Fas by FasL induces apoptosis by a mechanism that cannot be blocked by Bcl-2 or Bcl-x(L). Proc Natl Acad Sci U S A 1999;96:14871-14876.
25. Fujita E, Egashira J, Urase K, Kuida K, Momoi T. Caspase-9 processing by caspase-3 via a feedback amplification loop in vivo. Cell Death Differ 2001;8:335-344.
26. Deveraux Q, Reed J. IAP family proteins—suppressors of apoptosis. Genes Dev 1999;13:239-252.
27. Jost P, Grabow S, Gray D, McKenzie M, Nachbur U, Huang D, et al. XIAP discriminates between type I and type II FAS-induced apoptosis. Nature 2009;460:1035-1039.
28. Holler N, Zaru R, Micheau O, Thome M, Attinger A, Valitutti S, et al. Fas triggers an alternative, caspase-8-independent cell death pathway using the kinase RIP as effector molecule. Nat Immunol 2000;1: 489-495.
29. Degterev A, Huang Z, Boyce M, Li Y, Jagtap P, Mizushima N, et al. Chemical inhibitor of nonapoptotic cell death with therapeutic potential for ischemic brain injury. Nat Chem Biol 2005;1:112-119.
30. Baines C, Kaiser R, Purcell N, Blair N, Osinska H, Hambleton M, et al. Loss of cyclophilin D reveals a critical role for mitochondrial permeability transition in cell death. Nature 2005;434:658-662.
31. Caserta T, Smith A, Gultice A, Reedy M, Brown T. Q-VD-OPh, a broad spectrum caspase inhibitor with potent antiapoptotic properties. Apoptosis 2003;8:345-352.
32. Wei M, Zong W, Cheng E, Lindsten T, Panoutsakopoulou V, Ross A, et al. Proapoptotic BAX and BAK: a requisite gateway to mitochondrial dysfunction and death. Science 2001;292:727-730.
33. Walter D, Schmich K, Vogel S, Pick R, Kaufmann T, Hochmuth F, et al. Switch from type II to I Fas/CD95 death signaling on in vitro culturing of primary hepatocytes. HEPATOLOGY 2008;48:1942-1953.
34. Schmich K, Schlatter R, Corazza N, Ferreira KS, Ederer M, Brunner T, et al. Tumor necrosis factor α sensitizes primary murine hepatocytes to Fas/CD95-induced apoptosis in a Bim- and Bid-dependent manner. HEPATOLOGY 2011;53:282-292.
35. Cardier JE, Schulte T, Kammer H, Kwak J, Cardier M. Fas (CD95, APO-1) antigen expression and function in murine liver endothelial cells: implications for the regulation of apoptosis in liver endothelial cells. FASEB J 1999;13:1950-1960.
36. Baskin-Bey E, Washburn K, Feng S, Oltersdorf T, Shapiro D, Huyghe M, et al. Clinical Trial of the Pan-Caspase Inhibitor, IDN-6556, in Human Liver Preservation Injury. Am J Transplant 2007;7:218-225.
37. Pockros P, Schiff E, Shiffman M, McHutchison J, Gish R, Afdhal N, et al. Oral IDN-6556, an antiapoptotic caspase inhibitor, may lower aminotransferase activity in patients with chronic hepatitis C. HEPATOLOGY 2007;46:324-329.